



OPEN Assessment of *Mycobacterium tuberculosis* dodecin scaffold as a multimerization platform on the immunogenicity of HPV L2 antigens

Ecem Kaplan¹, Filipe Colaco Mariz¹, Xueer Zhao¹, Michelle Nessling², Lara Veitl¹, Yueru Zhang¹, Heiko Weyd¹ & Martin Müller¹✉

Human papillomavirus infection, the primary cause of cervical cancer (the fourth most common cancer in women), is preventable through prophylactic HPV vaccines. As an alternative to current HPV vaccines, all based on a cocktail of L1 virus-like particles (VLPs) from multiple HPV types, the L2 capsid protein offers cross-protection via a conserved epitope residing at the N-terminus between residues 20–38. The Trx-L2_(20–38)-8mer (Trx-8mer) is an L2-based antigen composed of a polytope of L2_(20–38) epitopes from eight HPV types inserted into thioredoxin from the hyperthermophilic archaeon *Pyrococcus furiosus* as a scaffold. We designed multivalent nanoparticle forms of Trx-8mer by using a dodecin protein from *Mycobacterium tuberculosis* (mtDod) assembling into dodecameric nanoparticles as a multimerization platform. Here, we explored two approaches to form dodecameric Trx-8mer nanoparticles: (i) direct fusion of the Trx-8mer to mtDod at the DNA level and (ii) decoration of mtDod nanoparticles after assembly with the Trx-8mer via the protein glue DogTag/DogCatcher. The reaction between Tag and Catcher results in isopeptide bond formation; thus, the covalent decoration of mtDod particles with the cargo (Trx-8mer) occurs. Despite the formation of nanoparticles by direct genetic fusion, this approach did not offer superior immunogenicity compared with the reference antigen, a heptameric form of the Trx-8mer. However, we showed that the decoration of assembled DogTag-mtDod nanoparticles with the cargo yielded the final antigen with a significant increase in immunogenicity with the induction of high neutralizing and cross-neutralizing antibody titers upon injection to BALB/c mice. We think that the lower immunogenicity observed with the direct genetic fusion of Trx-8mer to mtDod may be attributed to structural constraints affecting the accessibility of L2 epitopes to B cell receptors. Taken together, our final antigen obtained by decoration of DogTag-mtDod with DogCatcher-Trx-8mer holds potential as a multivalent L2-based antigen candidate for next-generation prophylactic HPV vaccines.

Human papillomavirus (HPV) has been recognized as an etiological agent for cervical cancer and genital warts since the early 1980s, following the detection of HPV 16 DNA in cervical cancer tissue and HPV 6 and 11 DNA in genital warts^{1–3}. Today, twelve of the HPV types are classified as human carcinogens, and another eight are classified as possibly/probably carcinogenic by the World Health Organization (WHO)⁴. Even though the immune system of immunocompetent individuals is able to clear most HPV infections within two years, persistent infection leads to productive cervical intraepithelial neoplasia 1 (CIN1, considered low-grade intraepithelial lesions, LSIL) or CIN2 and CIN3 high-grade intraepithelial lesions (HSIL). CIN3 precancerous lesions are at risk of progression to squamous-cell carcinoma or adenocarcinoma^{5,6}. Furthermore, HPV has been identified as a causative agent for other anogenital cancers^{7,8}, oropharyngeal cancers⁹ and is also suspected to play a role in skin cancers, particularly those associated with the cutaneous HPV types from the genus beta^{10,11}.

Six licensed prophylactic HPV vaccines, Gardasil[®] (2006), Cervarix[™] (2007), Gardasil 9[®] (2014), Cecolin[®] (2022, nationally licensed), Walrinvax[®] (2022, nationally licensed) and Cervavac[®] (nationally licensed)^{12–14} are

¹Tumorvirus-specific Vaccination Strategies, German Cancer Research Center (DKFZ), Heidelberg, Germany.

²Central Unit Electron Microscopy, German Cancer Research Center (DKFZ), Heidelberg, Germany. ✉email: martin.mueller@dkfz-heidelberg.de

all based on virus-like particle (VLP) antigens formed by the self-assembly of 360 HPV L1 capsid proteins. VLPs are produced in either insect or yeast cells or in *E. coli*. The prophylactic mechanism of HPV vaccines relies on the induction of neutralizing antibodies. Although the magnitude of the neutralizing antibody titers required for protection is not yet known, the safety and efficacy of the current vaccines have been proven^{15–17}. The neutralizing anti-L1 antibodies are raised against the hypervariable surface-exposed loops of L1 VLPs^{5,18,19}. Therefore, the current vaccines offer very limited cross-protection against nonvaccine HPV types²⁰. Owing to the limited cross-protection conferred by L1-based vaccines, inclusion of multiple HPV types in vaccine formulations is necessary to broaden the protection. The complexity of the formulation makes the vaccine manufacturing process costly. The requirement for a cold chain imposes additional logistical difficulties and limits accessibility²¹. Several efforts have made HPV vaccines more affordable to spread vaccination coverage worldwide, and the unit vaccine price has been reduced in low-income countries²². Despite these efforts, cervical cancer remains a burden, especially in sub-Saharan Africa and India^{7,23}.

In contrast to L1, the L2 protein, even though being less conserved than the L1 protein, exhibits superior cross-protection ability because of the presence of a conserved epitope residing at the N-terminus between residues 20–38^{24,25}. Hence, L2-based antigens have the potential for the production of broad protective HPV vaccines. When used in a vaccine, the immunogenicity of the linear L2 epitope must, however, compete with the robust immunogenicity of the highly ordered, repetitive VLP structures formed by L1. In the presented study, multimeric L2 antigens were designed to mimic this repetitive structure and improve immunogenicity. Multimerization of antigens is a well-established approach to enhance immunogenicity by inducing B-cell receptor cross-linking and triggering B-cell activation and proliferation^{17,26,27}. Our group has developed an L2-based antigen based on L2_(20–38) epitopes from eight different HPV types connected via a Gly-Gly-Pro (GGP) linker (designated L2_(20–38)-8mer or 8mer) and grafting 8mer into the surface-exposed active site of a thioredoxin scaffold derived from the hyperthermophilic archaea *Pyrococcus furiosus* (designated PfTrx-L2_(20–38)-8mer or Trx-8mer)²⁵. Furthermore, in the final antigen, PANHPVAX, the Trx-8mer was heptamerized through fusion with the OVX313 domain, further enhancing immunogenicity^{28,29}. PANHPVAX is currently being evaluated in a phase I clinical trial (EudraCT No. 2021 002584-22).

In this study, we aimed to develop an L2 antigen with greater valency than PANHPVAX to enhance the immunogenicity of the Trx-8mer by employing the mtDod multimerization platform. MtDod is an 8 kDa dodecin protein from *Mycobacterium tuberculosis* that is capable of self-assembling into hollow spherical dodecameric structures with 23-cubic symmetry and is stabilized via salt bridges between adjacent subunits. MtDod nanoparticles can accept and display 12 to 24 peptides with the aid of surface-exposed N- and C-termini. The very high thermal stability of mtDod enables the thermal purification of mtDod fusion proteins^{30,31}. In this work, the mtDod protein was fused to a Trx-8mer either by direct fusion at the DNA level or via DogTag/DogCatcher protein glue at the protein level. DogTag/DogCatcher is derived from the RrgA 4 domain of the adhesin protein of *Streptococcus pneumoniae*, which features a spontaneously forming isopeptide bond between lysine (Lys) and asparagine (Asn) residues, catalyzed by glutamic acid (Glu). This protein was split into 23 amino acid DogTag (Asn) and 104 amino acid DogCatcher (Lys and Glu) parts, which react by forming an isopeptide bond with each other in vitro³². We used this system to produce DogTag-mtDod and DogCatcher-Trx-8mer separately and combine these two components after purification. Next, we evaluated the B-cell response elicited upon immunization with mtDod-based L2 antigens and found that the leading candidate is obtained via decoration of mtDod nanoparticles with Trx-8mer proteins by using the DogTag/DogCatcher system. This antigen surpasses the heptameric Trx-8mer with respect to induction of (cross-) neutralizing antibodies targeting high-risk HPV types.

Results

Trx-8mer fusion to mtDod enables high-yield and purity antigen production

The first strategy for loading the mtDod scaffold with the L2 cargo involved the direct genetic fusion of the Trx-8mer to either the N- or C-terminus of mtDod (Fig. 1a). Here, the mtDod multimerization platform was evaluated alongside the OVX313 platform, which is known to enable heptamerization of the Trx-8mer²⁹. Additionally, a further mtDod-supported multimerized antigen, Trx-8mer-I5-mtDod, was designed by inserting the T-helper cell epitope I5 (VCGEVAYIQSVVSDCHVPTA) between the C-terminus of Trx and the N-terminus of mtDod. The T-helper epitope, I5, is also present within the OVX313 heptamerization platform as described previously^{29,33}.

The mtDod antigens were expressed in *E. coli*. Due to the exceptional thermal stability of mtDod at elevated temperatures up to 95 °C, the purification was carried out initially by thermal treatment to remove bacterial host proteins. The resulting supernatant, containing the soluble target protein, was then subjected to cation exchange chromatography (CEX) for further purification (Supplementary Fig. 1a-c). Salt bridges between mtDod subunits increase the stability of mtDod nanoparticles. Thus, a mixture of monomeric (Fig. 1b, yellow arrow) and multimeric forms (Fig. 1b, green arrow) of mtDod proteins can be observed by SDS-PAGE analysis after the treatment of samples with Laemmli sample buffer followed by heating at 95 °C for 10 min. To completely disassemble mtDod multimers, the samples were treated with a two-step sample preparation protocol: samples were mixed with buffer 1 and heated at 95 °C for 8 min followed by mixing with buffer 2 and heated at 95 °C for an additional 7 minutes³⁰ (See Fig. 1b part 1 and Supplementary Fig. 1.). Notably, compared with the C-terminal fusion, the fusion of the Trx-8mer to the N-terminus of dodecin led to a slightly lower expression level and reduced protein yield after purification (Supplementary Fig. 1a-b).

Multimerization of mtDod loaded with Trx-8mer, which is 30 kDa, was evaluated by using size exclusion chromatography (SEC), dynamic light scattering (DLS), and transmission electron microscopy (TEM).

Characterization of the antigens with SEC (Fig. 2a), DLS (Fig. 2b) and EM (Fig. 2c) consistently revealed the formation of multimeric nanoparticles. The SEC chromatogram shows that Trx-8mer-mtDod and Trx-8mer-I5-

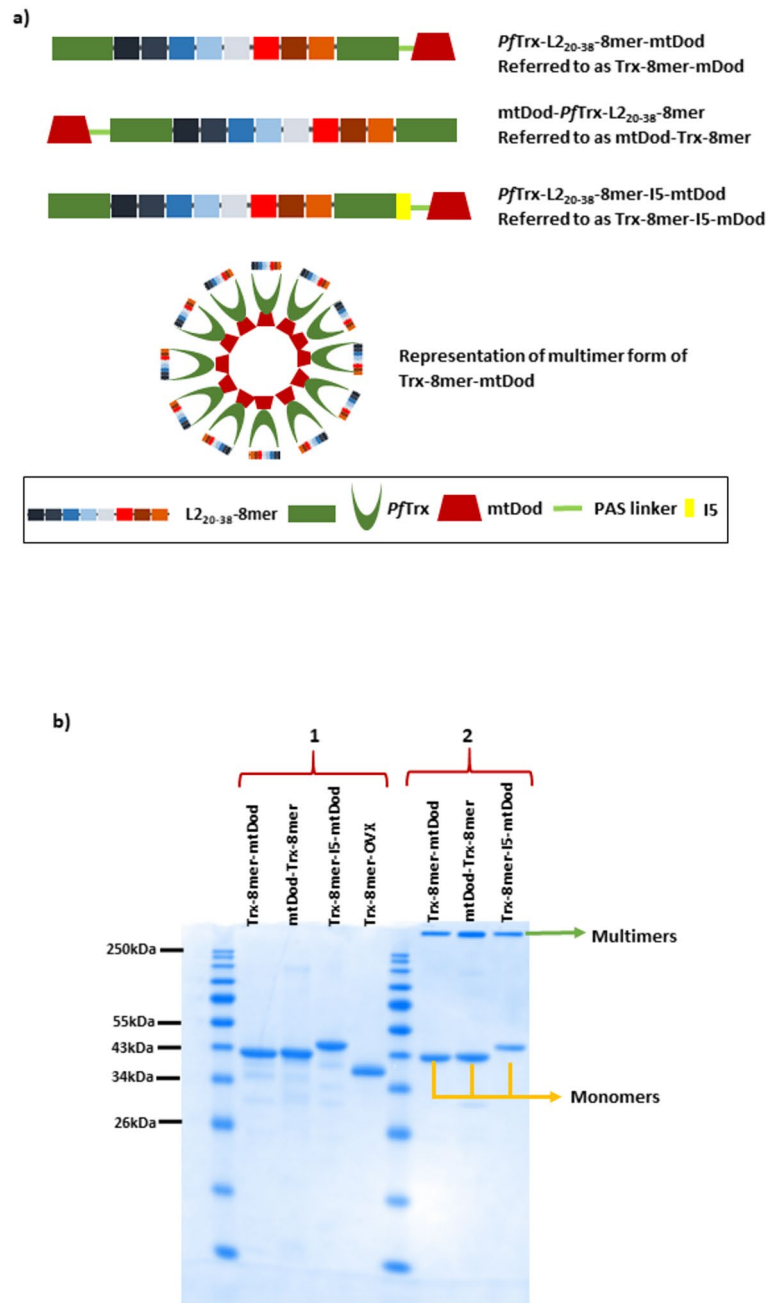


Fig. 1. Production of Trx-8mer antigens as fusion to mtDod. **(a)** Design of mtDod antigens as a fusion of the Trx-8mer with mtDod. mtDod: dodecin protein from *Mycobacterium tuberculosis* that forms dodecameric multimers, L2₂₀₋₃₈ 8mer: the combination of L2₂₀₋₃₈ epitopes from eight different HPV types (16–18–31–33–35–6–51–59), that were selected based on sequence homology to the major cross-neutralization HPV16 L2₂₀₋₃₈ epitope. The 8mer polytope was inserted into the active center of the Trx scaffold to generate the Trx-8mer. A rigid proline-alanine-serine (PAS) linker connects mtDod to the rest of the protein. **(b)** SDS-PAGE analysis comparing the purity of mtDod antigens with Trx-8mer-OVX (PANHPVAX), used as a reference antigen for immunization. To completely disassemble the multimeric mtDod antigens, samples (1) were treated using a two-step sample preparation protocol. A mixture of monomeric and multimeric mtDod proteins (2) were obtained when samples were treated with a single-step protocol.

mtDod antigens assemble into complexes with a molecular weight of approximately 443 kDa, which is consistent with the estimated molecular weight of the dodecamer. We observed that two distinct structures formed when the Trx-8mer was fused to the N-terminus of mtDod (Fig. 2a). EM imaging revealed hollow spherical particles approximately 8–9 nm in diameter, whereas DLS analysis estimated a hydrodynamic diameter of 22–29 nm. This discrepancy between TEM and DLS may arise from the differences in the fundamental measurement principles of the two techniques. DLS analysis might be affected by potential interparticle interactions³⁴. To our knowledge,

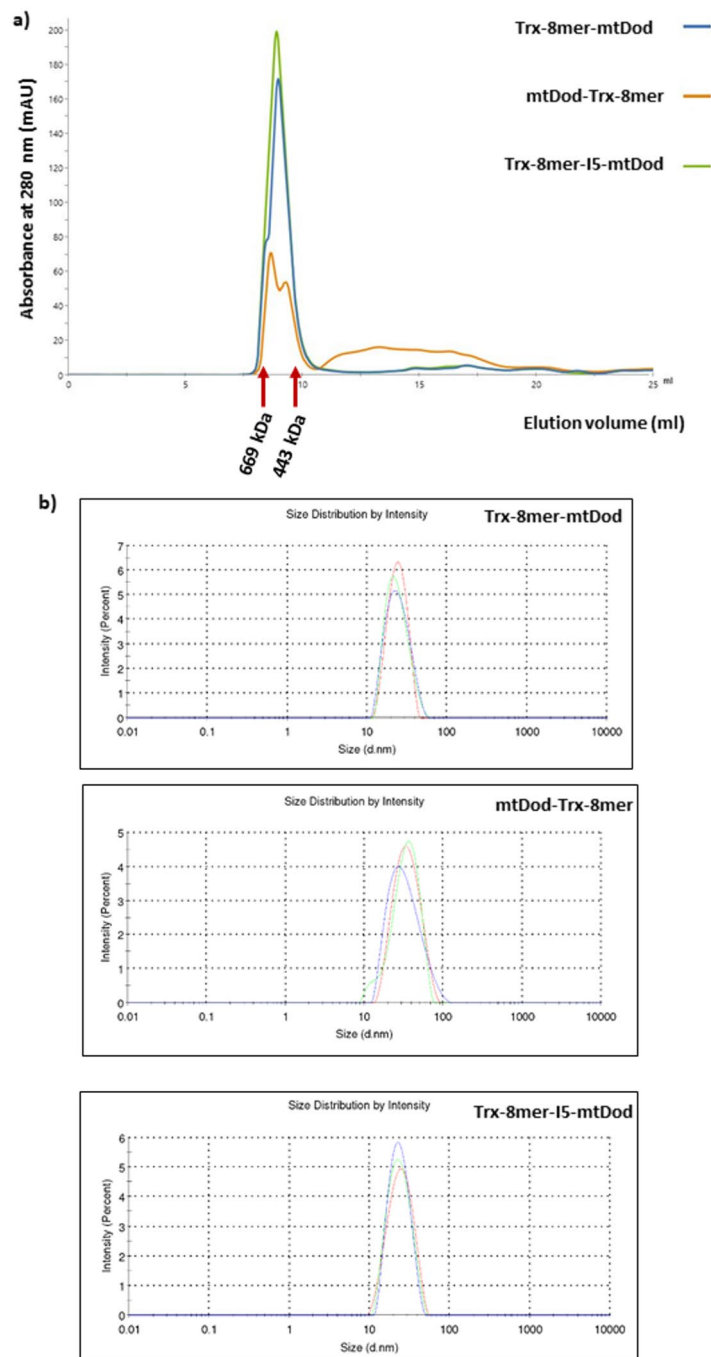


Fig. 2. MtDod particles form multimers when loaded with Trx-8mer cargo. **(a)** SEC analysis of purified proteins in comparison with the standard proteins (Gel Filtration Calibration Kit HMW, Cytiva) by using a Superdex 200 increase GL 20/300 column indicating the formation of multimers by mtDod fusion proteins (Gel Filtration Calibration Kit HMW, Cytiva: thyroglobulin (669 kDa), APO ferritin (443 kDa)). **(b)** DLS analysis of mtDod antigens. Trx-8mer-mtDod size (diameter in nm, d.nm): 24.8 ± 8.2 , Z-average (d.nm): 23.4, PDI: 0.168; mtDod-Trx-8mer size (d.nm): 34.8 ± 16.6 , Z-average (d.nm): 28.8, PDI: 0.154; Trx-8mer-I5-mtDod size (d.nm): 24.0 ± 6.9 , Z-average (d.nm): 22.1, PDI: 0.103. **(c)** The morphology of the nanoparticles was analyzed via EM. The red arrows indicate the nanoparticles after purification and endotoxin removal. Trx-8mer-mtDod, mtDod-Trx-8mer, Trx-8mer-I5-mtDod. The scale bar represents 50 nm.

there is no report showing the oligomerization of either mtDod-based dodecameric particles or *Pyrococcus furiosus* thioredoxin. However, dimerization of human thioredoxin has been previously described³⁵. To explore the potential for interparticle interactions, we used AlphaFold to model both monomeric and dimeric forms of Trx-8mer-mtDod (data not shown). The predicted structure of the Trx-8mer-mtDod dodecamer revealed that the mtDod domain forms the central core of the assembly, while the 8mer domains extend outward. Thioredoxin

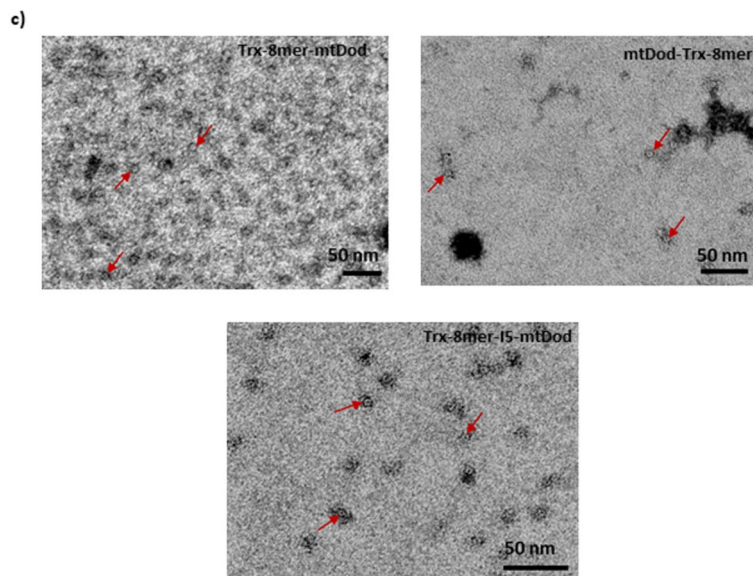


Fig. 2. (continued)

is embedded within the flexible regions of the 8mer domain, limiting its accessibility and reducing the likelihood of dimerization. Notably, the position and structural organization of mtDod in our model closely resemble that of OVX313 in the PANHPVAX construct, which also forms a central core (unpublished data). Furthermore, no previous studies on OVX313-multimerized Trx-L2 proteins have reported evidence of dimer formation²⁸. Due to AlphaFold's limitation in modeling proteins larger than 5000 residues, we modeled only the dimeric Trx-mtDod dodecamers. However, the predictions showed very low interface predicted template modelling (ipTM) and predicted template modelling (pTM) scores and this may indicate that there's not reliable dimeric formation between two dodecamers in nature.

Taken together, structural modeling and previous experimental data support the conclusion that these particles exist predominantly as dodecamers. In addition, the yield and purity of the antigens were sufficient to proceed with subsequent steps.

MtDod scaffold is decorated with Trx-8mer antigens mediated by isopeptide bond formation between DogTag and Catcher

An alternative strategy to display the Trx-8mer antigen on mtDod multimers involves the decoration of mtDod nanoparticles with a protein glue such as the DogTag/DogCatcher system³². Upon simple mixing, the tag and catcher form a spontaneous covalent bond, making it a powerful tool for site-specific Trx-8mer display on mtDod particles. We designed DogTag-mtDod (Fig. 3a) and DogCatcher-Trx-8mer (Fig. 3a) with the fusion of the DogTag peptide and DogCatcher to the N-terminus of mtDod and Trx-8mer, respectively. Both constructs could be produced in a soluble form in *E. coli* (Fig. 3c).

DogTag-mtDod nanoparticles illustrated in Fig. 3b were decorated with DogCatcher-Trx-8mer according to the reaction scheme presented in Fig. 3d. Isopeptide bond formation between DogTag and DogCatcher is evident in the SDS-PAGE gel image (Fig. 3e). The anti-DogTag antibody detects only the unreacted DogTag-mtDod, potentially due to the disruption of the DogTag epitope upon isopeptide bond formation with DogCatcher. The anti-DogTag blot clearly shows that the DogTag-mtDod reactant is consumed only in the presence of a DogCatcher component (Rxn1), providing additional evidence for the specificity of the reaction.

L2 antigens displayed on the mtDod platform elicit type-specific and cross-reactive neutralizing antibodies

Our previous data showed that the OVX313 heptamerization platform in PANHPVAX enhanced the immunogenicity of the Trx-8mer, resulting in stronger protection against both the vaccine and cross-type HPVs in both mice and guinea pigs²⁹. Based on this information, the mtDod platform, as a novel vaccine multimerization platform, was evaluated for enhanced immunogenicity. First, we aimed to investigate the B-cell response in terms of the production of HPV-neutralizing antibodies upon immunization with the two mtDod antigens Trx-8mer-mtDod and mtDod-Trx-8mer in comparison with PANHPVAX (Fig. 4a). To that end, mice were primed and subsequently boosted three times with 20 µg of antigens administered intramuscularly. A pseudovirion-based neutralizing assay (PBNA) was employed to measure the neutralizing antibody titers in the sera of mice collected one month after the last immunization.

Compared with the mtDod-Trx-8mer, immunization with Trx-8mer-mtDod resulted in higher neutralizing antibody titers (Fig. 4b). Notably, in mice receiving mtDod-Trx-8mer, neutralizing antibody titers remained below the threshold value for all tested PsV types in at least half of the mice. We did not further investigate the

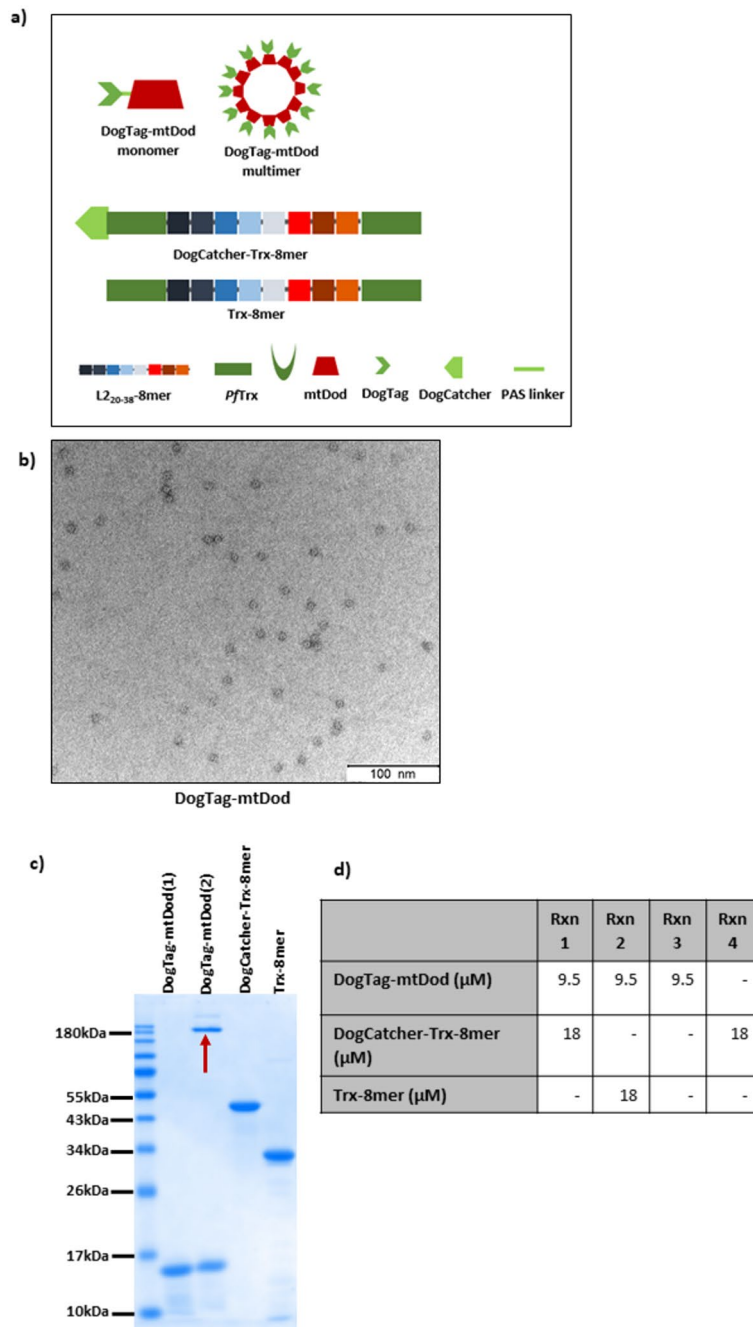


Fig. 3. MtDod scaffold can be decorated with Trx-8mer antigens via isopeptide bond formation between DogTag and DogCatcher. **(a)** Design of the components of the system and the Trx-8mer. **(b)** EM analysis of DogTag-mtDod. The red arrows indicate the 7 nm DogTag-mtDod nanoparticles. **(c)** SDS-PAGE analysis showing the purity of DogTag-mtDod (11 kDa) following anion exchange chromatography and SEC; DogCatcher-Trx-8mer (45 kDa) after purification with affinity chromatography and SEC; and Trx-8mer monomer (29 kDa) purified via thermal treatment. DogTag-mtDod is seen either as completely dissociated to monomeric units (1) or as a mixture of monomers and multimers (2). **(d)** Design of reactions (Rxn). **(e)** SDS-PAGE analysis of the reaction between DogTag-mtDod and DogCatcher-Trx-8mer. Conjugation can be detected by appearance of a band of higher molecular weight (~56 kDa) along with the consumption of reactants. Rxn2 is a control in which DogTag-mtDod and Trx-8mer are mixed. Rxn3 and Rxn4 are additional controls containing one reaction component under identical conditions. T: DogTag-mtDod and C: DogCatcher-Trx-8mer. The conjugates are marked with red arrows. **(f)** Western blot analysis confirming the reaction between Tag-Catcher using the primary antibodies anti-Trx, anti-DogTag, and anti-DogCatcher (Uncropped versions of images are depicted in Supplementary Fig. 3).

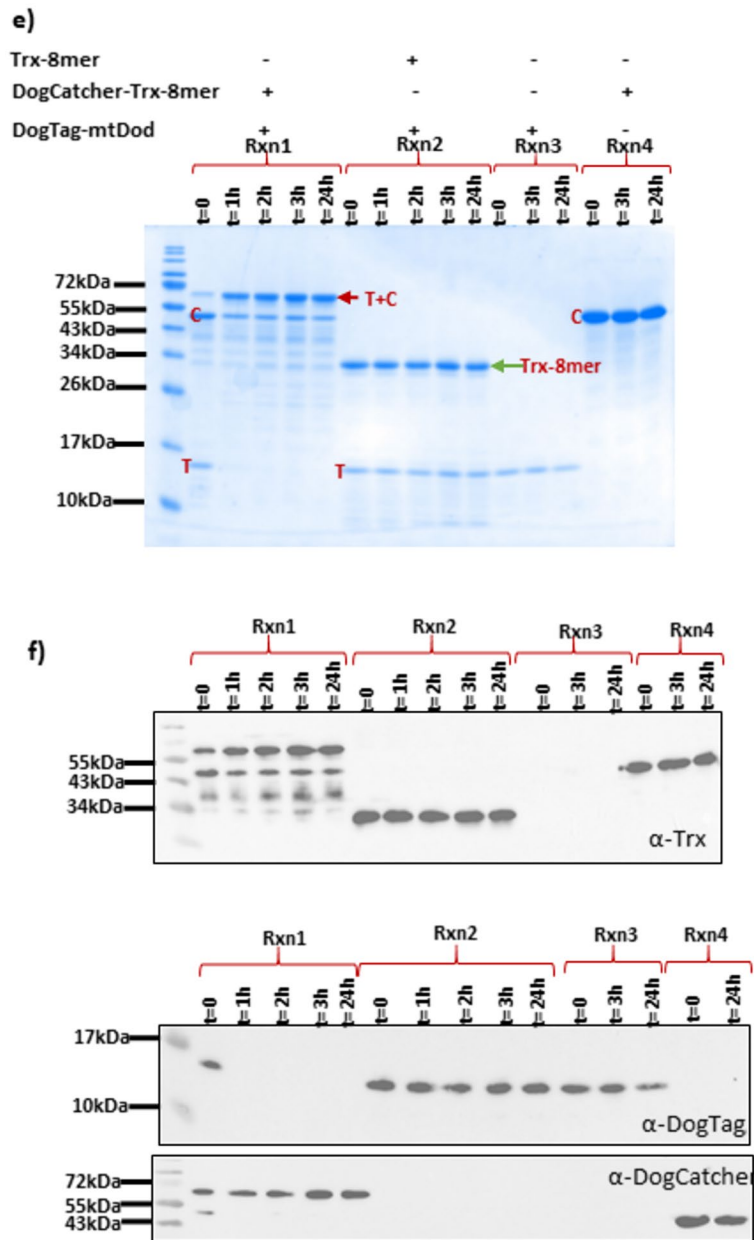


Fig. 3. (continued)

potential reasons for this result and continued with Trx-8mer-mtDod as the leading mtDod antigen candidate for subsequent experiments, given its superior immunogenicity and production yield (see Supplementary Fig. 1).

MtDod, as a vaccine platform, exposes the Trx-8mer polytope on the surface to induce neutralizing antibodies against vaccine types (HPV 16, HPV 18) and nonvaccine types (HPV 45 and HPV 58) upon immunization. Notably, only two and one of the mice immunized with Trx-8mer-mtDod, adjuvanted with SWE and AddaVax, respectively, demonstrated neutralizing ability against HPV 31. Low neutralizing antibody titers for HPV 31 have been reported in other studies^{29,36}. In contrast to the initial hypothesis, PANHPVAX vaccination induced approximately 6-fold and 3-fold higher neutralizing antibody titers against HPV 16 and HPV 18, respectively, compared to Trx-8mer-mtDod. A similar trend is observed for the other types, leading to the questions of what factors, beyond the multimerization status, might contribute to the superiority of PANHPVAX and how the immunogenicity of mtDod antigens can be enhanced. The latter is addressed with further experiments.

Additionally, we wanted to investigate the impact of two different adjuvants on the immunogenicity of Trx-8mer-mtDod: AddaVax™ and Sepivac SWE™, both of which are squalene-based oil-in-water emulsions, MF59-biosimilars and were previously employed in the formulation of influenza vaccines^{37,38}. AddaVax has been the adjuvant routinely used in our laboratory; however, the SWE adjuvant is suitable for clinical use and might offer an advantage in potential future clinical tests of mtDod antigens. As depicted in Fig. 4b, compared

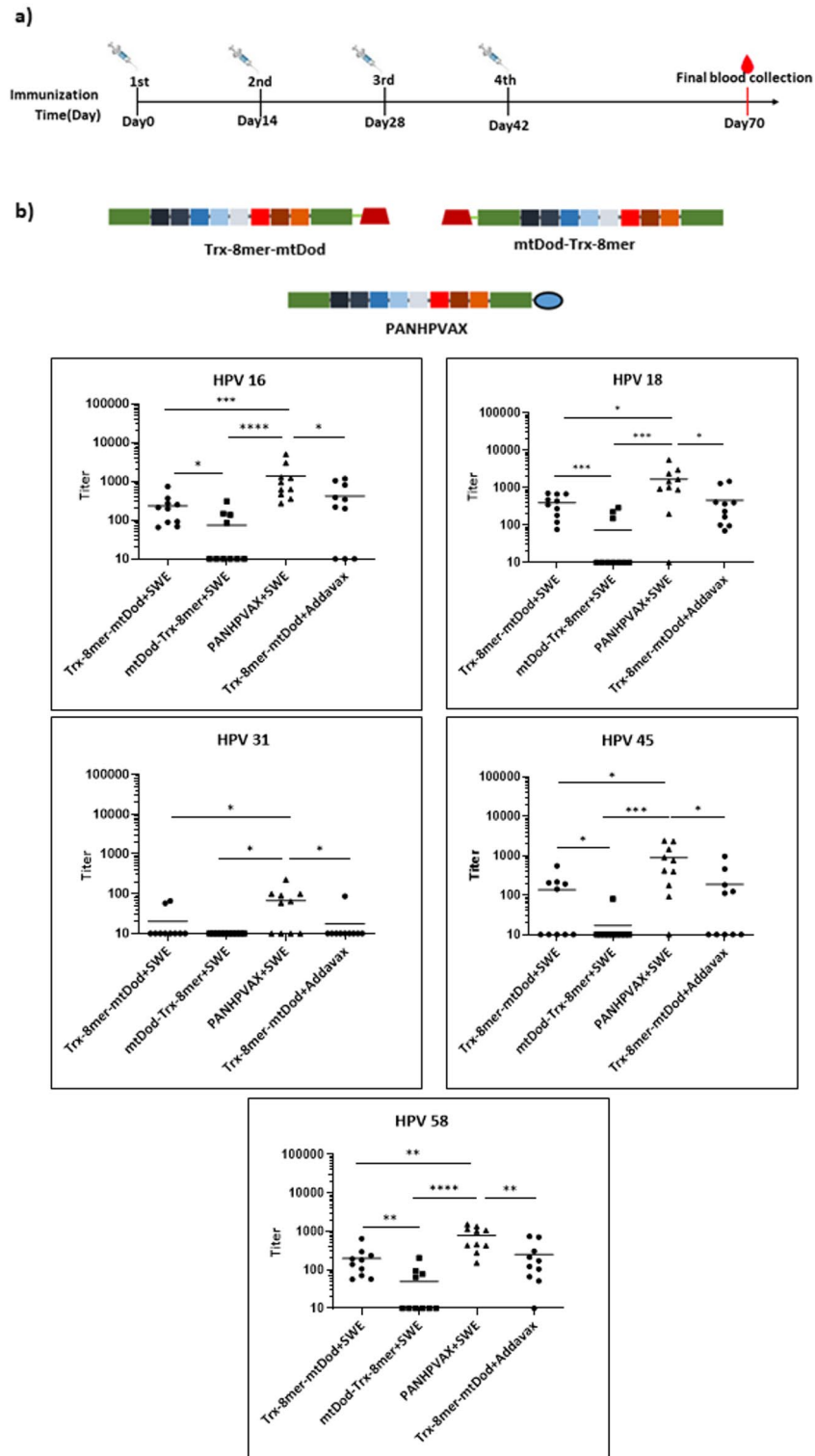


Fig. 4. L2 epitopes are accessible on Trx-8mer-mtDod multimers to induce type-specific and cross-neutralizing antibodies. **(a)** Immunization schedule. Six- to eight-week-old female BALB/c mice were immunized biweekly. **(b)** Sera collected from immunized mice ($n = 10$ mice per group) were tested for neutralizing antibodies by PBNA. The y-axis shows the serum neutralizing antibody titers as EC50 values. Each symbol represents the neutralizing antibody titer for one mouse. The horizontal lines indicate the means of the titers for each group. Statistical significance was evaluated by using a nonparametric Mann-Whitney test. A p value of ≤ 0.05 was considered significant. P values are as follows: < 0.05 , * < 0.01 , *** < 0.001 , **** < 0.0001 .

with AddaVax, the SWE adjuvant offers comparable immunogenicity to Trx-8mer-mtDod; therefore, the SWE adjuvant was used for subsequent immunizations.

Insertion of the T helper epitope I5 does not affect the immunogenicity of mtDod-L2 antigens

The incorporation of the OXV platform into vaccines might increase B-cell responses not only by multimerization but also by eliciting a T helper response due to the I5 T-cell epitope within OVX313^{28,29,39}. To account for this effect, we designed Trx-8mer-I5-mtDod (Fig. 1a) and evaluated the neutralizing antibody responses following vaccination with Trx-8mer-mtDod and Trx-8mer-I5-mtDod (Fig. 5a, b).

The data presented in Fig. 5b indicate that the additional T helper cell epitope in the Trx-8mer-I5-mtDod antigen does not offer improved immunogenicity compared to the Trx-8mer-mtDod antigen. Consistently, the anti-I5-specific T-cell response, as evaluated by IFN- γ ELISpot, revealed no significant differences between the different groups (data not shown). However, we do not have any experimental data for the processing and presentation of I5 epitope in the scope of this paper. Possibly, the location of the I5 peptide and flanking amino acids affect the processing of the peptide.

Anti-mtDod scaffold antibodies do not influence the induction of anti-L2 antibodies

We observed the presence of anti-mtDod antibodies in the sera of the mice immunized with Trx-8mer-mtDod (Fig. 6a), and we analyzed whether these antibodies negatively interfered with the immunogenicity of the 8mer. Anti-scaffold antibodies may neutralize the antigen at the time of the boost with Trx-8mer-mtDod^{40,41}. To investigate the influence of pre-existing scaffold antibodies on the titers of anti-L2 antibodies, one group of mice received DogTag-mtDod as the first dose, whereas a second control group received PBS. Both groups were subsequently boosted with Trx-8mer-mtDod (Fig. 6b). As shown in Fig. 6c, the presence of anti-mtDod antibodies at the time of Trx-8mer-mtDod injection did not diminish the neutralizing antibody titers against HPV 16 and 18. In contrast, mice without pre-existing anti-mtDod antibodies (PBS pre-immunization) showed a tendency to lower neutralizing antibody titers against HPV 16, compared to the group pre-immunized with mtDod. Taken together, we did not find evidence that pre-existing anti-mtDod antibodies would suppress the B-cell response against L2 epitopes in our studies.

A heterologous prime-boost regimen using PANHPVAX and Trx-8mer-mtDod shows no advantage over homologous PANHPVAX

Various studies have explored heterologous vaccination strategies. Combining DNA and protein vaccines elicited robust immune responses in HIV vaccine studies and SARS-CoV-2 vaccine studies, respectively^{42–44}. Furthermore, Bhattacharya et al. 2024 demonstrated the benefit of the heterologous application of two distinct protein scaffolds to present the SARS-CoV-2 receptor-binding domain (RBD) antigen⁴¹. In the presented study, we, therefore, explored the effect of incorporating PANHPVAX into the vaccination regimen of mtDod antigens. To this end, two heterologous immunization groups, one with PANHPVAX prime followed by Trx-8mer-mtDod boost and the other with the reverse order, were compared with the homologous immunization regimen consisting of either Trx-8mer-mtDod or PANHPVAX alone (Figure 7a).

Compared with homologous immunization with Trx-8mer-mtDod, a significant increase in the immune response elicited by heterologous immunization is evident from the HPV 16-PBNA and HPV 18-PBNA results (Fig. 7b). Mice that received a PANHPVAX prime/Trx-8mer-mtDod boost exhibited anti-HPV 16 neutralizing antibody titers that were five-fold of those measured in the mice receiving only Trx-8mer-mtDod. Furthermore, in the HPV 31 PsV neutralization assay, 5 out of 10 mice neutralized HPV 31 in the heterologous antigen groups, whereas this proportion is only 1 out of 10 in the homologous Trx-8mer-mtDod group. It is noteworthy that the sequence of antigen administration influences the final neutralizing antibody titers. Priming with PANHPVAX followed by Trx-8mer-mtDod boost resulted in a tendency for higher antibody titers than the reverse order. Despite the benefit of a heterologous immunization regimen over homologous Trx-8mer-mtDod immunization, it does not surpass homologous PANHPVAX immunization.

L2 antigens elicit enhanced immunogenicity when decorated onto mtDod particles via DogTag/DogCatcher

Despite our strategies to enhance the immunogenicity of mtDod nanoparticle antigens, vaccination with PANHPVAX consistently induced higher immune responses. This led us to explore an alternative strategy to decorate mtDod nanoparticles with the Trx-8mer. The assembly of multimeric structures is a complex process that can easily be distorted by the fusion of an additional antigen cargo. Although it has been reported that mtDod can be loaded with a cargo four-fold its size, it has also been noted that not only the size of the cargo but also the amino acid composition might interfere with particle assembly³⁰. Therefore, we designed an alternative approach to direct fusion and fused mtDod to DogTag (Fig. 3a), which is only a 23 amino acid peptide (3 kDa), in contrast to the larger 30 kDa Trx-8mer. The successful assembly of DogTag-mtDod nanoparticles with an approximate size of 7 nm is shown in Fig. 3b. To decorate these DogTag-mtDod particles, the DogCatcher partner of DogTag was fused to the Trx-8mer, and these two components were mixed to form spontaneous isopeptide bonds between Tag and Catcher (Fig. 3e). We anticipated that all DogTag sites on mtDod would be conjugated with DogCatcher-Trx-8mer unless there was a steric hindrance to the reaction⁴⁵. However, SDS-PAGE and western blot analysis revealed the presence of residual unconjugated DogCatcher-Trx-8mer in the mixture, despite further purification attempts. Therefore, the final antigen consisted of a mixture of decorated mtDod particles with Trx-8mer (T + C) and free DogCatcher-Trx-8mer. The neutralizing antibody titers induced by immunization with gene-level versus protein-level multimerized Trx-8mer by mtDod were assessed in BALB/c mice (Fig. 8).

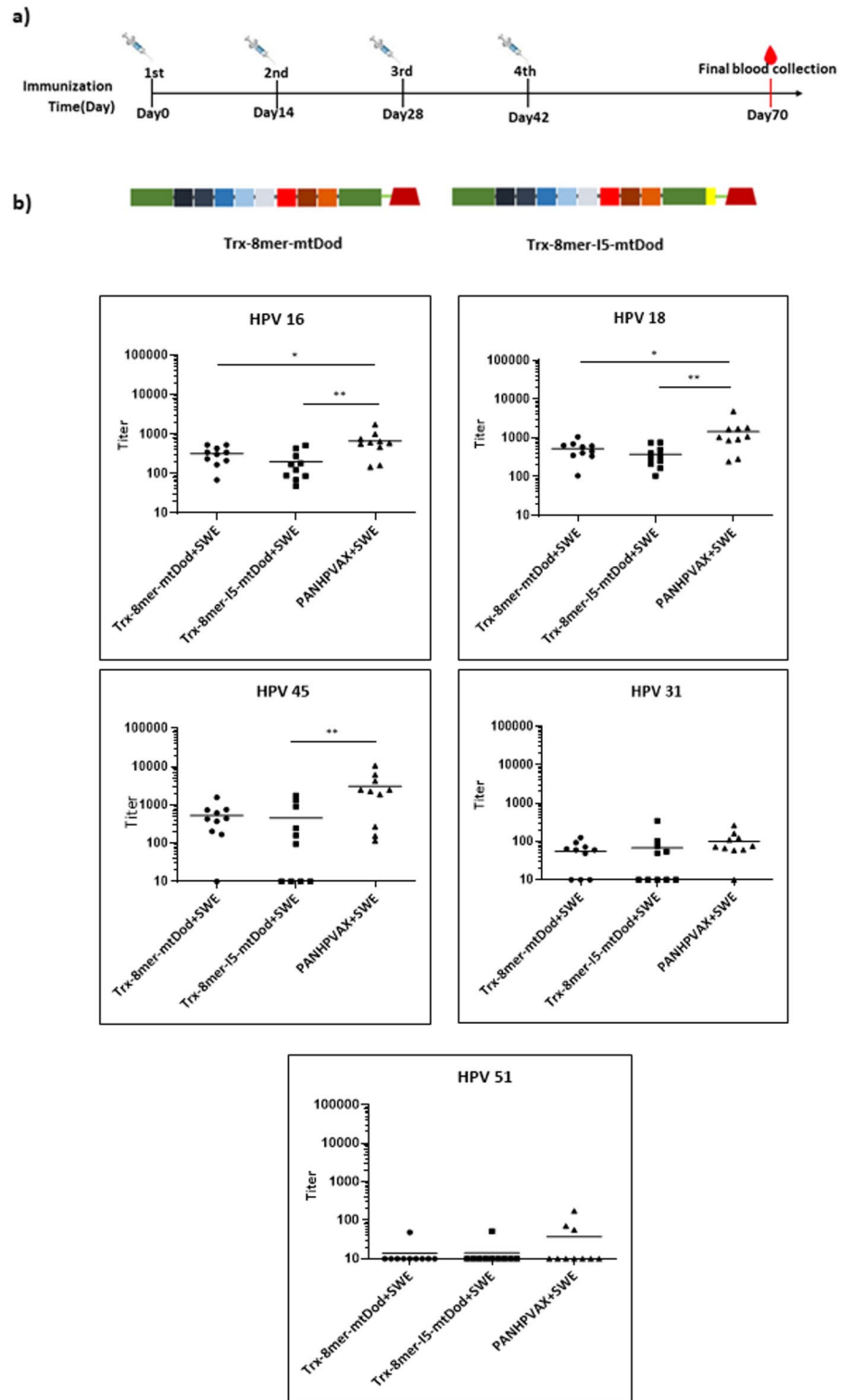


Fig. 5. Insertion of the I5 epitope does not improve B-cell responses induced by vaccination with Trx-8mer-mtDod. Six- to eight-week-old female BALB/c mice were immunized according to the schedule shown in (a). (b) Sera collected from immunized mice ($n = 10$ per group) were tested for neutralizing antibodies by PBNA. The y-axis shows the serum neutralizing antibody titers as EC50 values. Each symbol represents the neutralizing antibody titer for one mouse. The horizontal lines indicate the means of the titers for each group. A p value of ≤ 0.05 was considered significant. The p values are as follows: * < 0.05 , ** < 0.01 , *** < 0.001 , **** < 0.0001 .

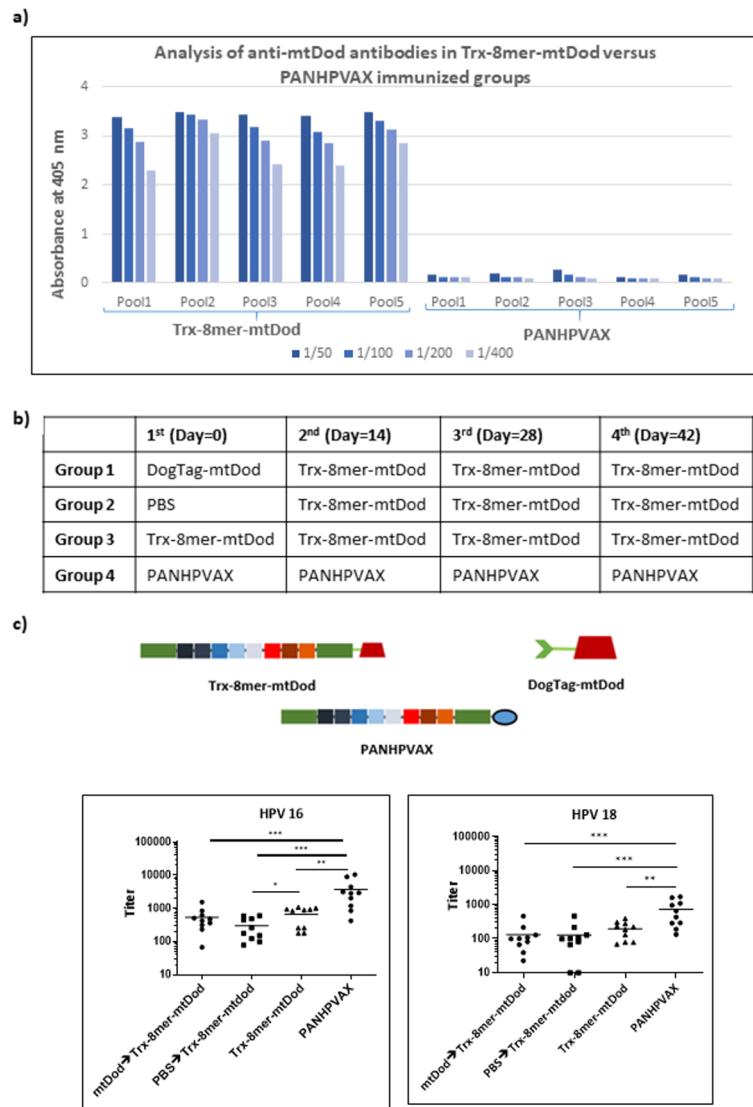


Fig. 6. Anti-mtDod scaffold antibodies do not impair the induction of neutralizing anti-L2 antibodies. **(a)** Anti-mtDod antibodies are raised following immunization with the Trx-8mer-mtDod antigen, as measured by ELISA. Each pool is composed of two serum samples. **(b)** Design of the groups to test the potential interference of anti-mtDod antibodies. Group 1 (mtDod \rightarrow Trx-8mer-mtDod) received DogTag-mtDod (lacking Trx-8mer) as the first dose (pre-immunization) whereas Group 2 (PBS \rightarrow Trx-8mer-mtDod) received only PBS as the first dose. Both groups were subsequently immunized three times with Trx-8mer-mtDod. Two additional groups were immunized four times with either Trx-8mer-mtDod (Group 3) or PANHPVAX (Group 4). **(c)** Sera collected from immunized mice ($n = 10$ mice per group) were tested for neutralizing antibodies by PBNA. The y-axis shows the serum neutralizing antibody titers as EC50 values. Each symbol represents the neutralizing antibody titer for one mouse. The horizontal lines indicate the means of the titers for each group. A p value of ≤ 0.05 was considered significant. The p values are as follows: * <0.05 , ** <0.01 , *** <0.001 , **** <0.0001 .

Figure 8b shows that, compared with the Trx-8mer-mtDod fusion, the decoration of mtDod nanoparticles after assembly with Trx-8mer (Trx-8mer-mtDod (T + C)) drastically improved the immunogenicity of the Trx-L2 antigen. Notably, this improved response was observed despite only approximately 50% of the Trx-8mer in the T + C group being present in the multimeric form, whereas the unconjugated DogCatcher-Trx-8mer remained in the monomeric form (Supplementary Fig. 5). Vaccination with Trx-8mer-mtDod (T + C) elicits 12-fold and 2-fold greater neutralizing antibody titers against HPV 16 compared to vaccination with Trx-8mer-mtDod and PANHPVAX, respectively. Likewise, the group receiving Trx-8mer-mtDod (T + C) exhibited five-fold higher HPV 18 neutralizing antibody titers compared to the group receiving gene-level fusion of Trx-8mer to mtDod. Furthermore, the former showed a tendency to neutralize HPV 18 PsVs better than PANHPVAX. Only one of the 10 mice vaccinated with Trx-8mer-mtDod could neutralize HPV 31, whereas this ratio reached 8 out of the 10 mice in the group that received Trx-8mer-mtDod (T + C), showing performance comparable to that of PANHPVAX. Additionally, cross-protective immunogenicity against HPV 45 was improved upon vaccination

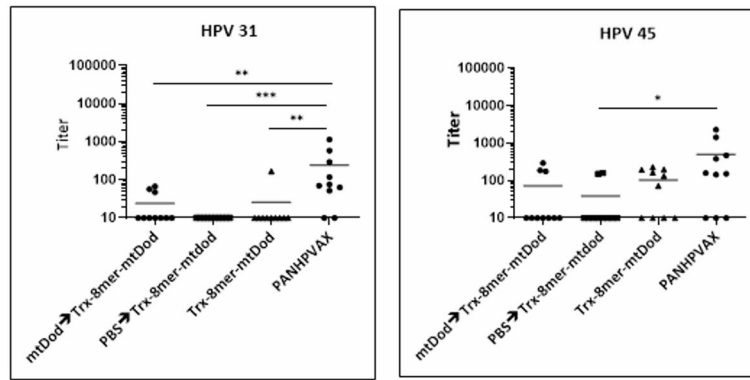


Fig. 6. (continued)

with Trx-8mer-mtDod (T + C) antigen compared to Trx-8mer-mtDod. Neutralizing antibody titers against HPV 39 were close to the lower threshold ($EC_{50} = 50$) in both the PANHPVAX and Trx-8mer-mtDod (T + C) groups, whereas they fell below the threshold in mice immunized with Trx-8mer-mtDod. Immunization with Trx-8mer-mtDod (T + C) and PANHPVAX elicited comparable responses against other high-risk HPV types, including HPV 52 and 58, while titers remained significantly lower in the Trx-8mer-mtDod group.

Next, we evaluated the potential boosting effect of DogTag/DogCatcher on the immunogenicity of Trx-8mer-mtDod (T + C). In this case, not only anti-L2 antibodies but also anti-mtDod antibodies should be boosted in this group. To test this hypothesis, anti-mtDod antibody titers (EC_{50}) were compared in the sera of the mice in the Trx-8mer-mtDod and Trx-8mer-mtDod (T + C) groups (Fig. 8c). However, anti-mtDod antibody titers remained the same in both antigen groups, indicating the lack of a boosting effect of DogTag/DogCatcher.

Our findings showed the benefit of covalently adding Trx-8mer molecules onto assembled mtDod particles. We believe that this benefit may arise from the antigen structure. It is possible that the Trx-8mer cargo, when directly fused to the mtDod at genetic level, is too large and interferes with the proper assembly of mtDod multimers. TEM analysis of Trx-8mer-mtDod particles (Fig. 2c) revealed a similar morphology to that of DogTag-mtDod (Fig. 3b); however, these images (Fig. 2c) do not provide insight into Trx-8mer display. Trx-8mer-mtDod (T + C) may facilitate better spatial arrangement of Trx-8mer molecules.

Discussion

Numerous follow-up studies since the introduction of the L1 protein-based HPV vaccines in 2006 and 2007 have provided strong evidence for the efficacy and safety of the commercially available HPV vaccines. Neutralizing antibody titers remain durable for over a decade, supporting long-term vaccine efficacy⁴⁶. Recent efforts— such as dose reduction⁴⁶ and antigen production in the economically feasible host *E. coli* (Cecolin™)⁴⁷— have contributed to increased accessibility of HPV vaccines. Despite an increasing number of WHO member states introducing the HPV vaccine into their national immunization programs, globally, only 27% of girls have received at least one dose⁴⁸. Here, our group focuses on an HPV L2 protein-based, thermostable HPV vaccine antigen with the main goal of producing a more affordable and accessible vaccine, particularly in low- and middle-income countries where most cervical cancer cases occur. In our study, we used an L2-based vaccine antigen, Trx-8mer, which has been designed as a Thioredoxin Displayed Muropeptide Immunogen (TDMI)²⁵. Thioredoxin from *Pyrococcus furiosus*, PfTrx, is a scaffold that lacks cross-reactivity with human Trx⁴⁹. Previous research has shown the thermal stability of PfTrx, enabling easier production of the antigen by thermal purification⁴⁹. A related product, PANHPVAX, a heptamerized form Trx-8mer, is currently undergoing evaluation in a phase 1 clinical trial (EU CT number: 2024–511493-67-00).

The prophylactic efficacy of an HPV vaccine strictly depends on the induction of neutralizing antibodies. One mechanistic explanation of initial B-cell activation is the BCR cross-linking model, which proposes that aggregation of the BCR is followed by immunoreceptor tyrosine-based activation motif (ITAM) accumulation and initiation of intracellular signaling⁵⁰. In this model, BCRs, binding to an antigen, cluster in close proximity, forming an “immunon” to trigger optimal B-cell signaling^{17,26}. Furthermore, BCR clustering promotes the internalization of antigens by BCR-dependent endocytosis followed by the presentation of antigenic peptides on MHC class II molecules for T-cell receptor (TCR) binding and T cell activation⁵¹. Based on the above-mentioned model, antigen multivalency is one of the key contributors to BCR clustering and subsequent events, explaining the high humoral immunogenicity of the current HPV vaccines, which are composed of highly repetitive structures (VLPs).

In the presented study, we evaluated the mtDod protein as a platform for the multimerization of L2-based HPV antigens. Previously, mtDod was employed to induce antibodies against peptides displayed on mtDod nanoparticles³⁰. To our knowledge, the only study employing mtDod as a vaccine platform for the multimerization of *Mycobacterium tuberculosis* antigens was conducted by Zhao and colleagues, who demonstrated that antigen multimerization significantly enhanced immunogenicity⁵².

Initially, we designed two mtDod antigens as a direct genetic fusion of the Trx-8mer to either the N- or the C- termini of mtDod to evaluate its potential as a dodecameric multimerization platform. These mtDod antigens

a)

	1 st (Day=0)	2 nd (Day=14)	3 rd (Day=28)	4 th (Day=42)
Group 1	PANHPVAX	Trx-8mer-mtDod	Trx-8mer-mtDod	Trx-8mer-mtDod
Group 2	Trx-8mer-mtDod	PANHPVAX	PANHPVAX	PANHPVAX
Group 3	Trx-8mer-mtDod	Trx-8mer-mtDod	Trx-8mer-mtDod	Trx-8mer-mtDod
Group 4	PANHPVAX	PANHPVAX	PANHPVAX	PANHPVAX

b)

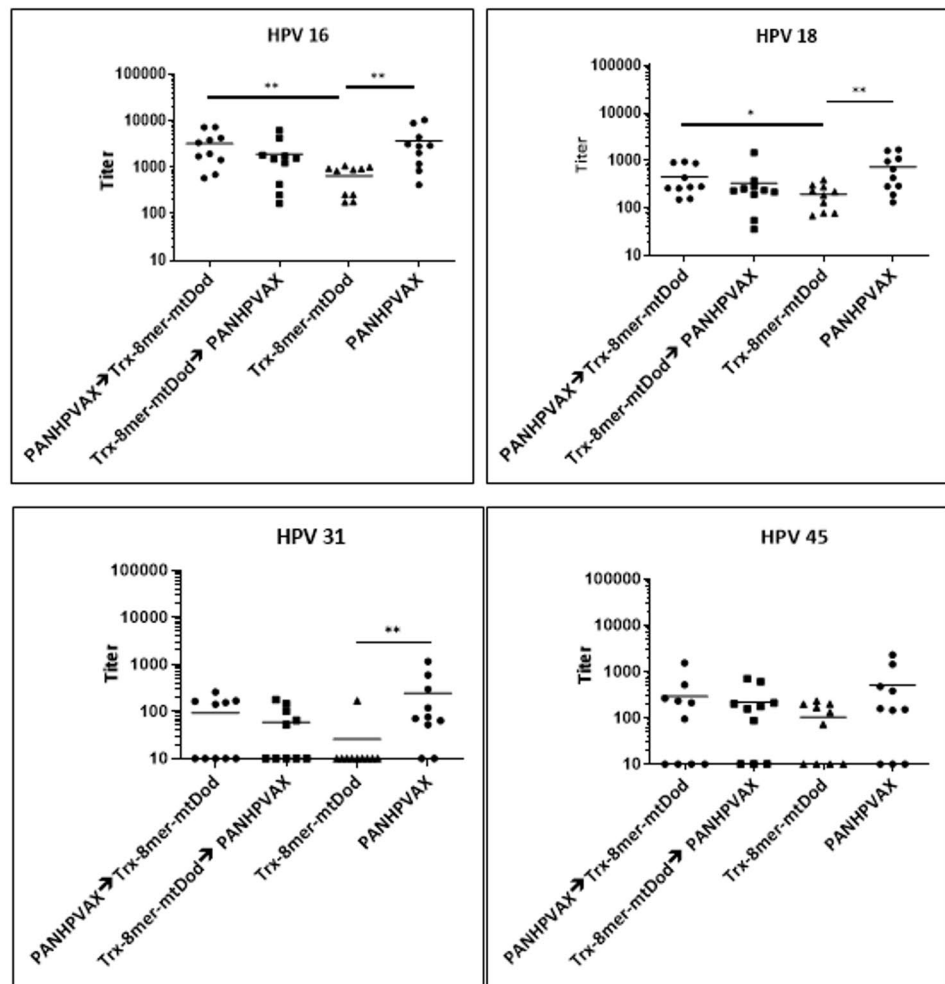
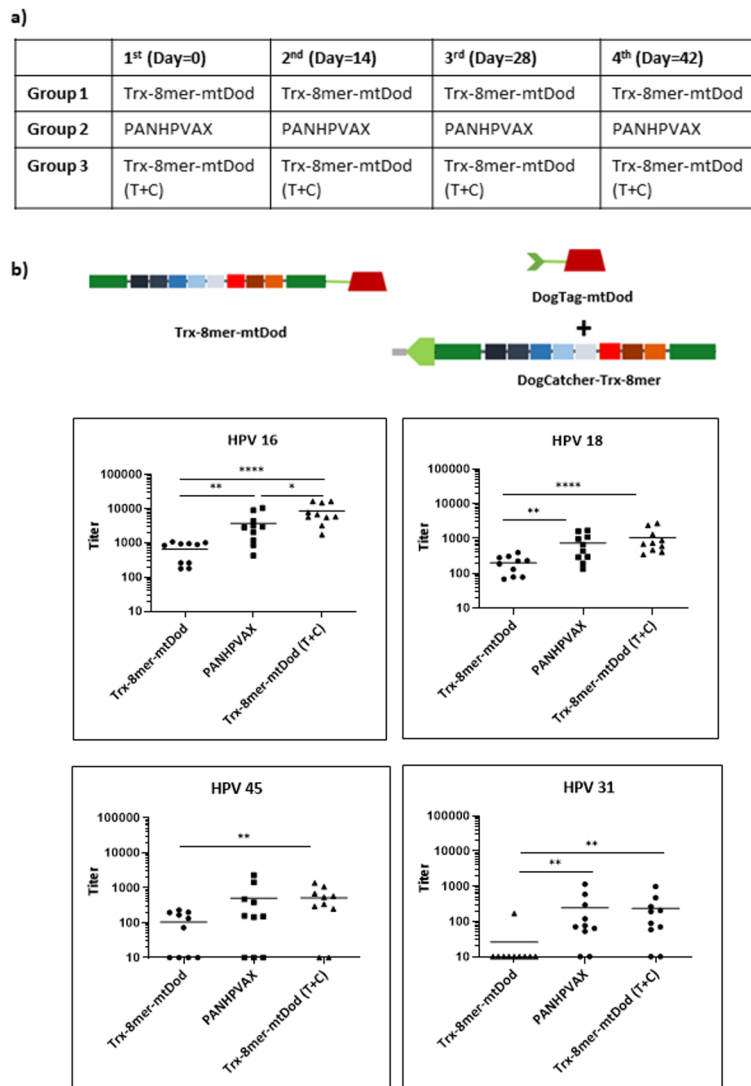


Fig. 7. Heterologous prime-boost with PANHPVAX and mtDod antigens induces comparable neutralizing antibody titers as the homologous PANHPVAX prime-boost group. (a) Immunization schedule of different vaccine combinations (Group 1: PANHPVAX-->Trx-8mer-mtDod, Group 2: Trx-8mer-mtDod--> PANHPVAX). (b) Sera collected from immunized mice ($n = 10$ mice per group) were tested for neutralizing antibodies by PBNA. The y-axis shows the serum neutralizing antibody titers as EC50 values. Each symbol represents the neutralizing antibody titer for one mouse. The horizontal lines indicate the means of the titers for each group. A p value of ≤ 0.05 was considered significant. The p values are as follows: * <0.05 , ** <0.01 , *** <0.001 , **** <0.0001 .



were easy to produce in *E. coli* with high yield and purity. Vaccination with mtDod antigens induced type-specific and non-vaccine type cross-neutralizing antibodies, but the immunogenicity of Trx-8mer multimerized with mtDod could not surpass that of the heptameric antigen PANHPVAX. We first sought to incorporate the T helper cell epitope in the heptamerization domain, OVX313^{11,28,29,33,53}, into the most promising mtDod-based antigen in order to induce additional T helper cell activation and thus augment B-cell responses. However, this modification did not enhance the immunogenicity of Trx-8mer-mtDod, which may be attributable to suboptimal processing and presentation of the T-helper cell epitope, although this was not further investigated within the scope of the present study.

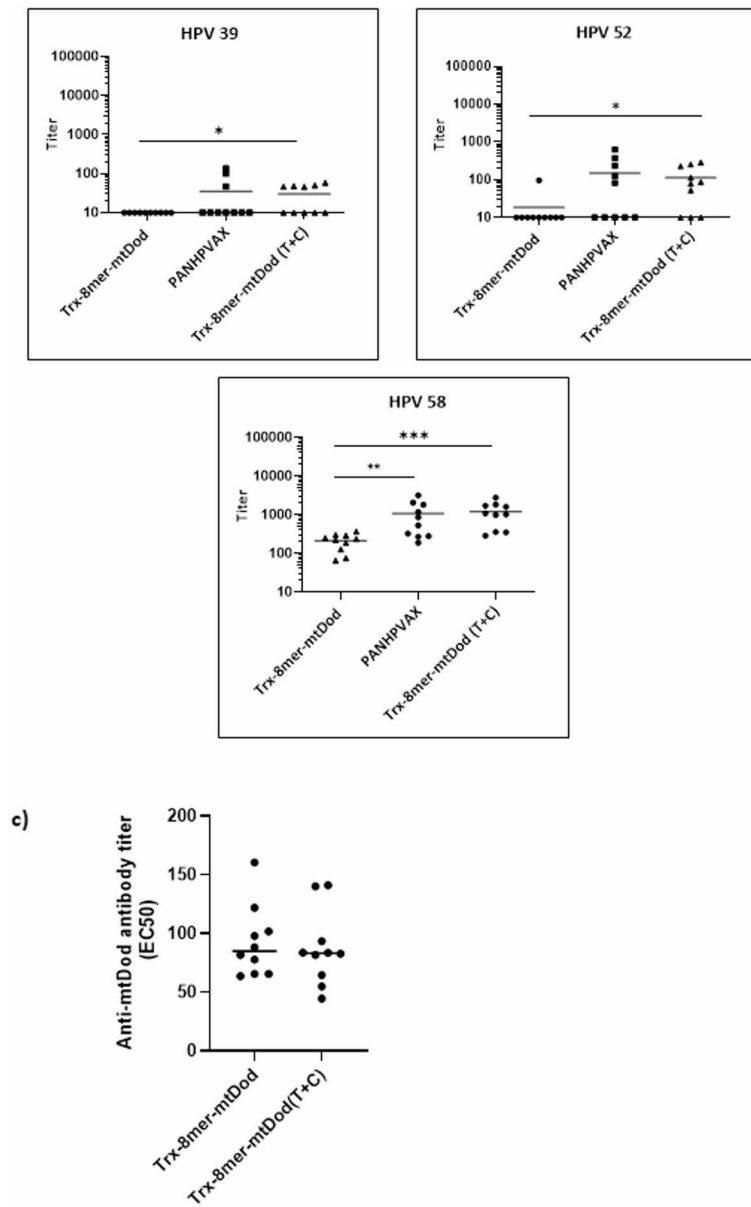


Fig. 8. (continued)

Taken together, we observed a diminished immunogenicity of the direct fusion of Trx-8mer to the C-terminus of mtDod (Fig. 4b), which indicates that the genetic fusion of Trx-8mer to mtDod may sterically interfere with proper particle folding and assembly and possibly also with the accessibility of the L2 epitopes.

Previously, Yang et al. reported diminished titers of anti-L2 antibodies following boosting due to the effect of anti-ferritin scaffold antibodies⁵⁴. As expected, we detected anti-mtDod scaffold antibodies in the sera after immunization with mtDod antigens; therefore, we investigated the effect of anti-scaffold antibodies on the L2 immune response in the prime-boost regimen. We showed that pre-existing anti-mtDod antibodies at the time of immunization with Trx-8mer-mtDod did not influence the induction of neutralizing antibody titers against the tested HPV types, possibly because of the immune dominance of L2 epitopes and lack of competition with the anti-scaffold antibodies^{27,55}.

We further investigated the benefit of a heterologous immunization approach. Compared with homologous vaccination, heterologous vaccination involving mtDod- and OVX313-L2 antigen combinations enhanced the induction of neutralizing antibodies against HPV types 16, 18, 45, and 31 PsVs. Based on our findings, the sequence of antigen administration influences the immune response, as priming with mtDod antigen followed by boosting with OVX313 antigen did not result in a significant improvement over the homologous regimen in contrast to the reverse sequence.

An alternative approach to recombinant fusion proteins is the combination of two protein units via covalent bonds using protein glue systems. These systems, such as SpyTag/SpyCatcher^{56,57}, SnoopTag/Catcher⁵⁸ and DogTag/DogCatcher³², are derived from bacterial proteins that naturally contain an internal isopeptide bond¹⁵⁹.

In our hands, a fusion of SpyTag to the N-terminus of mtDod resulted in an insoluble protein (data not shown). Therefore, we explored DogTag-mtDod as a modular scaffold to display DogCatcher-Trx-8mer molecules. The small size of DogTag enables its fusion to mtDod without interfering with the particle assembly. These particles were decorated with an equimolar amount of Trx-8mer existing in DNA level fusion Trx-8mer-mtDod. Only approximately 50% of the Trx-8mer in the DogTag/DogCatcher group was present in the multimeric form (Fig. 3e and Supplementary Fig. 5). Nevertheless, Trx-8mer molecules conjugated to mtDod via Tag/Catcher elicited significantly higher neutralizing antibody titers against all the tested PsVs than did the gene-level fusion of the Trx-8mer to mtDod (Trx-8mer-mtDod) (Fig. 8b). Moreover, we found that these particles were significantly more immunogenic than PANHPVAX against PsVs of the high-risk type HPV 16 (Fig. 8b).

With respect to this improved immunogenicity of Trx-8mer-mtDod (T + C), we addressed the question of whether the DogTag/DogCatcher pair itself offers a boosting effect; however, we did not find evidence for this scenario in our experiments (Fig. 8c). A further reason might be the structural advantage of this antigen, as site-specific conjugation of the Trx-8mer to assembled mtDod nanoparticles may ensure proper folding and orientation of the antigen. Moreover, in addition to enhanced BCR cross-linking, additional properties of the vaccine need to be considered, which may also induce more robust B-cell responses. It is likely that an increased particle size (Supplementary Fig. 2) might influence antigen kinetics, leading to prolonged antigen retention in lymph nodes, and, in turn, can affect the B cell response^{60,61}.

A limitation of our study to this end is the lack of a side-by-side comparison of electron microscopy images of Trx-8mer fused to mtDod at DNA level versus post-assembly decorated nanoparticles (Supplementary Fig. 4). Additionally, our study does not provide direct evidence for enhanced B cell activation induced by mtDod-mediated multimerization, such as upregulation of activation markers CD69 or CD86 on B cells *in vitro*, or on B cells analyzed *ex vivo*. However, previous data from our group have demonstrated a clear benefit of multimerized antigens compared with their monomeric form^{29,33}. Moreover, in another immunization setup, we tested the immunogenicity of monomeric Trx-8mer and we found that only five out of ten mice immunized with monomer raised neutralizing antibody titers against HPV 18; furthermore, in the same group, none of the mice exhibited a response above the threshold (neutralizing antibody titers lower than 50 were considered non-neutralizing) against HPV 31 (unpublished data).

In conclusion, our working hypothesis predicted that multimerized dodecamer mtDod-based antigens would elicit an improved B cell response compared with PANHPVAX. In accordance with this hypothesis, the data presented here provide evidence for successful optimization of the Trx-8mer antigen by multimerization on mtDod using DogTag/DogCatcher system. We propose this thermally stable antigen with robust immunogenicity as a promising candidate for next-generation HPV vaccines with the aim of improving global vaccine coverage, particularly in resource-limited settings. Beyond this, the modular design may enable further addition of HPV E7 epitopes for co-display with L2 epitopes on the same particle to combine prophylactic and therapeutic effects.

Materials and methods

Accordance statement

BALB/c mice were purchased from Janvier Labs, France and housed under pathogen-free conditions at the German Cancer Research Center (DKFZ) in compliance with German and European statutes. Mice were assigned to the groups randomly by animal care-takers who did not take part in the experiments. All animal experiments were carried out with the approval of the responsible Animal Ethics Committee of the Regional Council of Karlsruhe, Germany; 35–9185.81/G-139/21 and all methods were conducted in accordance with relevant guidelines and regulations. The animals were housed in the rooms with 12 h light/12 h dark cycle at 20–24 °C and 45–65% relative humidity. All animals were monitored daily by animal care-takers and no visible adverse effect of vaccination was observed.

Design of the constructs

Bacterial expression plasmids were designed to encode fusion proteins of mtDod to Trx-8mer or DogTag, besides the fusion of DogCatcher to Trx-8mer. The PAS linker (LESPAAPAPASPAS) was inserted between mtDod and the rest of the protein. To design Trx-8mer-I5-mtDod protein, I5 epitope (VCGEVAYIQSVVSDCHVPTA) was inserted between Trx and PAS linker. All expression plasmids were synthesized by GenScript. The Trx-8mer-OVX313 protein (PANHPVAX), which was used as a reference for immunization experiments, was produced by Biomeva GmbH as a GMP-compliant protein.

Protein expression and purification

All the recombinant plasmids encoding the target proteins were expressed in the *E. coli* BL21 strain. Protein production was performed in 400 ml of LB medium, including 25 µg/ml kanamycin, and the cultures were incubated at 37 °C and 200 rpm until the OD₆₀₀ reached 0.5–0.6. Subsequently, expression was induced with either 1 mM or 0.5 mM isopropyl β-D-1 thiogalactopyranoside (IPTG) overnight at room temperature with shaking at 140–160 rpm. The next day, the cells were harvested by centrifugation and resuspended in lysis buffer (buffer of mtDod proteins: 300 mM NaCl, 5 mM MgCl₂ and 20 mM Tris-HCl (pH 8.0), 0.16% Tween 20 and buffer for DogCatcher-Trx-8mer: 300 mM NaCl, 25 mM Tris-HCl (pH 8.0), 0.16% Tween 20). All the lysis buffers included 0.5 mM phenylmethylsulfonyl fluoride (PMSF) and a protease inhibitor tablet (cComplete™, EDTA-free protease inhibitor cocktail, Merck) to inhibit the activity of the cellular proteases. Cell lysis was performed with a French press, and the cleared lysate for further purification.

MtDod proteins were purified via thermal treatment before ion exchange chromatography for 20 min at 70 °C (Trx-8mer-mtDod, Trx-8mer-I5-mtDod, and mtDod-Trx-8mer) or 75 °C (DogTag-mtDod). The lysates were cooled on ice for 15 min and centrifuged at 15,000 rcf and 4 °C for 10 min. Trx-8mer-mtDod, Trx-8mer-I5-mtDod and mtDod-8mer-L2 were further purified via cation exchange chromatography (HiTrap SP-FE,

Cytiva), and anion exchange chromatography (HiTrap Q-FF, Cytiva) was used for DogTag-mtDod. Elution was performed with a linear NaCl gradient. The DogCatcher-Trx-8mer included six histidine residues at the N-terminus; therefore, it was purified via histidine affinity chromatography (HiTrap Chelating HP, Cytiva). Elution was performed with a linear imidazole gradient. The DogCatcher-Trx-8mer protein-containing fractions were pooled and polished with SEC following affinity chromatography. ÄKTA Pure 25 Chromatography System (Cytiva) was used for all elution steps.

Eluted fractions were analyzed with SDS-PAGE and the fractions containing a high amount of target protein were pooled and dialyzed against PBS (pH 7.4) and concentrated, if necessary, by using Amicon Ultra-15 Centrifugal Filter tubes (Amicon, Merck) for subsequent steps.

Proteins were detoxified to prevent interference from bacterial endotoxin contamination. The phase-separation method with 1% (v/v) Triton X-114 was used to remove endotoxin from the purified proteins. After endotoxin removal, the concentration of the target protein was determined in comparison with bovine serum albumin (BSA) standards with known concentrations on the same gel.

Size exclusion chromatography (SEC)

SEC was used to confirm the multimerization status of antigens or to polish purified antigens as a final purification step. Superdex 200 10/300 GL or HiLoad 200 16/600 columns were operated with ÄKTA Pure 25 FPLC system and Unicorn™ 7.8 software (Cytiva) according to the manufacturer's instructions. The samples were subsequently centrifuged at 15,000 rcf and 4 °C for 30 min before being injected into the SEC column. Either PBS or PBS with DTT was used as the mobile phase. One-milliliter fractions were collected during 1.5 CV elution and analyzed *via* SDS-PAGE. The retention times of the eluted proteins were compared with the retention times of the standard proteins to determine the molecular weights of the purified proteins.

Dynamic light scattering (DLS)

The dynamic light scattering (DLS) technique was used to measure the hydrodynamic size and analyze the polydispersity of the purified proteins. DLS analysis was performed via a Zetasizer DLS device (Malvern Panalytical) on a 1 ml sample in PBS, which was centrifuged at 15,000 rcf, 4 °C for 10 min and equilibrated at 25 °C. The measurements were performed in triplicate.

Formulation of the antigens and immunization

Six- to eight-week-old female BALB/c mice ($n = 10$ mice per group) were injected with the antigens as explained below. To test the humoral response induced by mtDod antigens, 20 µg of antigen was adjuvanted with 50% (v/v) SWE™ (Seppic) or AddaVax™ (InvivoGen) for immunization. Regarding the group of mtDod multimers decorated with Trx-8mer epitopes *via* the DogTag/DogCatcher system, instead of the total protein amount, the mole number of the Trx-8mer was calculated to be the same as that of the 20 µg of gene-level fusion of mtDod to Trx-8mer (Trx-8mer-mtDod). 50 µl of the formulated antigens were injected intramuscularly into the caudal thigh muscle four times at biweekly intervals. Final blood was collected by cardiac puncture one month after the last immunization and incubated overnight at 4 °C for coagulation, followed by centrifugation to collect the sera. Anesthesia was not applied to the mice in this study. Animals were euthanized by carbon dioxide inhalation prior to final blood collection. Immunizations were performed always with two people and one of them was also the experimenter measuring the responses. Therefore, experimenters were not blinded.

Pseudovirion preparation

Pseudovirions (PsVs) were prepared based on the protocol described previously with slight modifications^{29,62}. Production was performed in the human fibroblast line 293TT *via* co-transfection of humanized HPV L1 and L2 protein-encoding plasmids in addition to a reporter plasmid encoding Gaussia luciferase using GenJet™ *in vitro* DNA transfection reagent (SignaGen Laboratories). PsVs were purified with an OptiPrep (Sigma) gradient, which was an iodixanol-based solution.

Pseudovirion-based neutralization assay (PBNA)

Neutralizing antibody titers in the sera against various HPV types were tested by using the pseudovirion-based neutralization assay PBNA. Briefly, 50 µl sera, which were initially diluted 1:25 with complete DMEM, were titrated in 96-well plates. Next, 50 µl of diluted pseudovirus was added to the wells, and the serum-PSV mixture was incubated for approximately 20 min. Finally, 50 µl of a 2.5×10^6 HeLaT cells/ml cell suspension was added to the serum-PSV complex, and the plates were incubated at 37 °C with 95% humidity and 5% CO₂ for 48 h. The amount of secreted Gaussia luciferase was determined in 10 µl of the medium by using Gaussia-Glow Juice (PJK GmbH, Germany) according to the manufacturer's instructions. The luminescence signal was measured 15 min after the addition of the substrate by a Luminometer (Victor Nivo, PerkinElmer). The results were normalized against the infection control response that was present in each plate as a mixture of only PsVs and cells. The serum neutralizing antibody titer (EC50) for each individual mouse was calculated as the reciprocal of the dilution of serum that inhibits PsV infection by 50% (EC50). EC50 values below 50 were considered as non-neutralizing.

SDS-PAGE and western blot

SDS-PAGE was carried out on the Laemmli gel system by using either a 12.5% or 10% running gel. Before SDS-PAGE, mtDod proteins were subjected to a two-step denaturation protocol, including treatment with acidic loading buffer (4x buffer 1:10% (w/v) SDS and 300 mM acetic acid) at 95 °C for 8 min followed by treatment with loading buffer 2 (4x buffer 2: 50% (v/v) glycerol, 300 mM unbuffered Tris, 200 mM Tris-HCl pH 6.8, 10% (v/v) β-mercaptoethanol, 50 mM EDTA, bromophenol blue) at 95 °C for 10 minutes³⁰. In addition, to analyze a mixture of monomers/multimers, samples were mixed with Laemmli loading buffer (3x: 30% (v/v) glycerol,

6% (w/v) SDS, 15% (v/v) β -mercaptoethanol, 187.5 mM Tris-HCl pH 6.8, bromophenol blue) and heated at 95 °C for 10 min. The gels were either stained with Coomassie Brilliant Blue (GelCode™ Blue Safe Protein Stain, Thermo Fisher Scientific) or transferred to a membrane for western blotting. Gel images were taken by using Image Lab 3.0 software (Bio-Rad, USA).

The proteins on the gel were transferred to 0.2 μ m nitrocellulose membranes for immunoblotting (Trans-Blot Turbo™ Transfer System, Bio-Rad). The membranes were blocked with 5% skim milk in PBST (1x PBS containing 0.3% Tween 20) for 1 h at room temperature and incubated with primary antibodies (anti-Trx, anti-DogTag, and anti-DogCatcher) at 4 °C overnight. A goat anti-mouse IgG + IgM antibody conjugated to horseradish peroxidase (HRP) was used as a secondary antibody. A chemiluminescence signal was developed with a ChemiDoc Imaging System (Bio-Rad, USA) after the addition of HRP substrate (Clarity ECL Western Blotting Substrates, Bio-Rad).

DogTag-dogcatcher reactions

Isopeptide bond formation occurs between DogTag and DogCatcher upon mixing two components in a suitable buffer. The reactions were optimized in terms of the concentration of the reactants, reaction time, temperature and buffer. The concentration of DogCatcher-Trx-8mer was adjusted considering the L2 amount required for immunization, 9.5 μ M DogTag-mtDod and 18 μ M DogCatcher-Trx-8mer were mixed in PBS on ice, and the reaction was carried out at 4 °C. DogTag-mtDod was mixed with Trx-8mer without DogCatcher as a control. The reactions were analyzed by SDS-PAGE, and the mixture was stored at -20 °C until immunization.

GST-mtDod ELISA

F96 Polysorp, Nunc Immuno Plates (Thermo Fisher Scientific) were coated with glutathione casein (GC), which has a high affinity for glutathione-S-transferase (GST); therefore, the mtDod protein fused to GST (GST-mtDod) could bind to GCs. In this way, anti-mtDod antibodies in the serum could be detected. First, the plates were coated with 100 μ l/well GC diluted to 1:500 in coating buffer (50 mM carbonate buffer pH 9.6, 50 mM Na_2CO_3 , 50 mM NaHCO_3) and incubated at 4 °C overnight. The next day, the plates were washed three times with PBST and blocked with 150 μ l/well casein blocking buffer (PBS, 0.2% casein, 0.05% Tween 20) at 37 °C for 1 hour. GST-mtDod total lysate produced from *E. coli* BL21 was added to the plates at 100 μ l/well (0.75 μ g/ μ l) and incubated at 37 °C for 1 hour. Concurrently, serum had to be pre-incubated with only GST lysate to block the interference of any antibodies raised against bacterial proteins, and sera were diluted 1:50 in casein blocking buffer containing 3 μ g/ μ l GST lysate and incubated at room temperature for 1 hour. The plates were washed three times with PBST. Sera were titrated in the plates at 50 μ l/well final volume and incubated at room temperature for 1 hour. The plates were washed as described above and incubated with the secondary antibody goat anti-mouse-HRP (GAMPO) at 37 °C for 1 hour. Finally, the substrate 2,2'-azinobis (3-ethylbenzothiazoline-6-sulfonic acid) (ABTS) was added to the wells, and the absorbance of the product of the colorimetric reaction was measured at 405 nm.

Transmission electron microscopy (TEM)

The electron microscopy images were obtained by Dr. Michelle Neßling and Dr. Karsten Richter. MtDod multimers, DogTag-HPV 16-L1 capsomers and VLPs from purified preparations were adsorbed onto glow discharged carbon-coated copper grids (300 mesh, Science Services, Munich, Germany), washed in water (injectable-quality, Braun, Melsungen, Germany) and negatively stained with 1% aqueous uranyl acetate. Micrographs were taken with a Zeiss EM 910 at 80 kV (Carl Zeiss, Oberkochen, Germany) using a slow scan CCD camera (TRS, Moorenweis, Germany). The addition of scale bars and adjustment of the contrast on the images was performed via ImageJ software.

Statistical analysis

GraphPad Prism 10.1.0 (GraphPad Software, USA) was used to calculate the EC50 values for each serum from median of duplicates. A nonparametric Mann-Whitney test was performed to calculate statistical differences, and $p \leq 0.05$ was considered statistically significant.

Data availability

All the important data generated in the current study are provided in this manuscript and supplementary file. Additional detailed data can be requested from the first author or the corresponding author.

Received: 28 May 2025; Accepted: 26 February 2026

Published online: 13 March 2026

References

- Shah, K. H., Lewis, M. G., Jenson, A. B., Kurman, R. J. & Lancaster, W. D. Papillomavirus and cervical dysplasia.. *Lancet* [https://doi.org/10.1016/s0140-6736\(80\)92617-3](https://doi.org/10.1016/s0140-6736(80)92617-3) (1980).
- zur Hausen, H. Human genital cancer: Synergism between two virus infections or synergism between a virus infection and initiating events.. *Lancet* [https://doi.org/10.1016/s0140-6736\(82\)91273-9](https://doi.org/10.1016/s0140-6736(82)91273-9) (1982).
- Dürst, M., Gissman, L., Ikenberg, H. & zur Hausen, H. A papillomavirus DNA from a cervical carcinoma and its prevalence in cancer biopsy samples from different geographic regions. *Proc. Natl. Acad. Sci. U. S. A.* **80**, 3812–3815 (1983).
- A review of human carcinogens. IARC Monographs on the Evaluation of Carcinogenic Risks to Humans.* Vol. 100B: 1–441. (2012).
- Doorbar, J., Egawa, N., Griffin, H., Kranjec, C. & Murakami, I. Human papillomavirus molecular biology and disease association. *Rev. Med. Virol.* **25**, 2–23. <https://doi.org/10.1002/rmv.1822> (2015).
- zur Hausen, H. Papillomaviruses and cancer: From basic studies to clinical application. *Nat. Rev. Cancer.* **2**, 342–350. <https://doi.org/10.1038/nrc798> (2002).

7. de Martel, C., Plummer, M., Vignat, J. & Franceschi, S. Worldwide burden of cancer attributable to HPV by site, country and HPV type. *Int. J. Cancer* **141**, 664–670. <https://doi.org/10.1002/ijc.30716> (2017).
8. Silva, L. L. D. et al. Malignancy associated with low-risk HPV6 and HPV11: A systematic review and implications for cancer prevention. *Cancers (Basel)* <https://doi.org/10.3390/cancers15164068> (2023).
9. Hubbers, C. U. & Akgul, B. HPV and cancer of the oral cavity. *Virulence* **6**, 244–248. <https://doi.org/10.1080/21505594.2014.999570> (2015).
10. Harwood, C. A. et al. Human papillomavirus infection and non-melanoma skin cancer in immunosuppressed and immunocompetent individuals. *J. Med. Virol.* **61**, 289–297. [https://doi.org/10.1002/1096-9071\(200007\)61:3%3C289::aid-jmv2%3E3.0.co;2-z](https://doi.org/10.1002/1096-9071(200007)61:3%3C289::aid-jmv2%3E3.0.co;2-z) (2000).
11. Mariz, F. C. et al. A broadly protective vaccine against cutaneous human papillomaviruses. *npj Vaccines* **7**, 116. <https://doi.org/10.1038/s41541-022-00539-0> (2022).
12. Harper, D. M. & DeMars, L. R. HPV vaccines - A review of the first decade. *Gynecol. Oncol.* **146**, 196–204. <https://doi.org/10.1016/j.ygyno.2017.04.004> (2017).
13. Illah, O. & Olaitan, A. Updates on HPV vaccination. *Diagnostics (Basel)* <https://doi.org/10.3390/diagnostics13020243> (2023).
14. World Health Organization Prequalified vaccines [Internet], Accessed on 24.04.25 Available at: <<https://extranet.who.int/prequal/vaccines/prequalified-vaccines>>
15. Einstein, M. H. et al. Comparison of long-term immunogenicity and safety of human papillomavirus (HPV)-16/18 AS04-adjuvanted vaccine and HPV-6/11/16/18 vaccine in healthy women aged 18–45 years: End-of-study analysis of a Phase III randomized trial. *Hum. Vaccin. Immunother.* **10**, 3435–3445. <https://doi.org/10.4161/hv.36121> (2014).
16. Restrepo, J. et al. Ten-Year Follow-up of 9-Valent Human Papillomavirus Vaccine: Immunogenicity, Effectiveness, and Safety. *PEDIATRICS* **152** (2023).
17. Chackerian, B. & Peabody, D. S. Factors that govern the induction of long-lived antibody responses. *Viruses* <https://doi.org/10.3390/v12010074> (2020).
18. Schiller, J. T. & Muller, M. Next generation prophylactic human papillomavirus vaccines. *Lancet. Oncol.* **16**, e217–225. [https://doi.org/10.1016/S1470-2045\(14\)71179-9](https://doi.org/10.1016/S1470-2045(14)71179-9) (2015).
19. Godi, A., Vaghadia, S., Cocuzza, C., Miller, E. & Beddows, S. Contribution of surface-exposed loops on the HPV16 capsid to antigenic domains recognized by vaccine or natural infection induced neutralizing antibodies. *Microbiol. Spectr.* <https://doi.org/10.1128/spectrum.00779-22> (2022).
20. Ribeiro-Müller, L. & Müller, M. Prophylactic papillomavirus vaccines. *Clin. Dermatol.* **32**, 235–247. <https://doi.org/10.1016/j.clindermatol.2013.08.008> (2014).
21. Huber, B., Wang, J. W., Roden, R. B. S. & Kirnbauer, R. RG1-VLP and other L2-based, broad-spectrum HPV vaccine candidates. *J. Clin. Med.* <https://doi.org/10.3390/jcm10051044> (2021).
22. Gavi, T. V. A. Gavi Strategic Goal 4, Market Shaping Roadmap Human Papillomavirus Vaccines. (2023).
23. Stelzle, D. et al. Estimates of the global burden of cervical cancer associated with HIV. *Lancet. Glob. Health.* **9**, e161–e169. [https://doi.org/10.1016/S2214-109X\(20\)30459-9](https://doi.org/10.1016/S2214-109X(20)30459-9) (2021).
24. Gambhira, R. et al. A protective and broadly cross-neutralizing epitope of human papillomavirus L2. *J. Virol.* **81**, 13927–13931. <https://doi.org/10.1128/JVI.00936-07> (2007).
25. Rubio, I. et al. Potent anti-HPV immune responses induced by tandem repeats of the HPV16 L2 (20–38) peptide displayed on bacterial thioredoxin. *Vaccine* **27**, 1949–1956. <https://doi.org/10.1016/j.vaccine.2009.01.102> (2009).
26. Dintzis, H. M., Dintzis, R. Z. & Vogelstein, B. Molecular determinants of immunogenicity: The immunon model of immune response. *Proc. Natl. Acad. Sci. U.S.A.* **73**, 3671–3675 (1976).
27. Marcandalli, J. et al. Induction of potent neutralizing antibody responses by a designed protein nanoparticle vaccine for Respiratory Syncytial Virus. *Cell* **176**, 1420–1431 e1417. <https://doi.org/10.1016/j.cell.2019.01.046> (2019).
28. Spagnoli, G. et al. Broadly neutralizing antiviral responses induced by a single-molecule HPV vaccine based on thermostable thioredoxin-L2 multiepitope nanoparticles. *Sci. Rep.* <https://doi.org/10.1038/s41598-017-18177-1> (2017).
29. Pouyanfar, S. et al. Minor capsid protein L2 polytope induces broad protection against oncogenic and mucosal Human Papillomaviruses. *J. Virol.* <https://doi.org/10.1128/JVI.01930-17> (2018).
30. Bourdeaux, F. et al. Dodecin as carrier protein for immunizations and bioengineering applications. *Sci. Rep.* **10**, 13297. <https://doi.org/10.1038/s41598-020-69990-0> (2020).
31. Liu, F. et al. Structural and biophysical characterization of *Mycobacterium tuberculosis* dodecin Rv1498A. *J. Struct. Biol.* **175**, 31–38. <https://doi.org/10.1016/j.jsb.2011.04.013> (2011).
32. Keeble, A. H. et al. DogCatcher allows loop-friendly protein-protein ligation. *Cell Chem Biol* **29**, 339–350 e310, (2022). <https://doi.org/10.1016/j.chembiol.2021.07.005>
33. Zhao, X. et al. Combined prophylactic and therapeutic immune responses against human papillomaviruses induced by a thioredoxin-based L2-E7 nanoparticle vaccine. *PLoS Pathog.* **16**, e1008827. <https://doi.org/10.1371/journal.ppat.1008827> (2020).
34. Filippov, S. K. et al. Dynamic light scattering and transmission electron microscopy in drug delivery: A roadmap for correct characterization of nanoparticles and interpretation of results. *Mater. Horiz.* **10**, 5354–5370. <https://doi.org/10.1039/d3mh00717k> (2023).
35. Weichsel, A., Gasdaska, J. R., Powis, G. & Montfort, W. R. Crystal structures of reduced, oxidized, and mutated human thioredoxins: Evidence for a regulatory homodimer. *Structure* **4**, 735–751. [https://doi.org/10.1016/s0969-2126\(96\)00079-2](https://doi.org/10.1016/s0969-2126(96)00079-2) (1996).
36. Seitz, H. et al. A three component mix of thioredoxin-L2 antigens elicits broadly neutralizing responses against oncogenic human papillomaviruses. *Vaccine* **32**, 2610–2617. <https://doi.org/10.1016/j.vaccine.2014.03.033> (2014).
37. Kim, E. H. et al. Squalene emulsion-based vaccine adjuvants stimulate CD8 T cell, but not antibody responses, through a RIPK3-dependent pathway. *eLife* <https://doi.org/10.7554/eLife.52687> (2020).
38. Gao, F. et al. AddaVax-Adjuvanted H5N8 inactivated vaccine induces robust humoral immune response against different clades of H5 viruses. *Vaccines (Basel)* <https://doi.org/10.3390/vaccines10101683> (2022).
39. Schiller, J. T. & Lowy, D. R. Understanding and learning from the success of prophylactic human papillomavirus vaccines. *Nat. Rev. Microbiol.* **10**, 681–692. <https://doi.org/10.1038/nrmicro2872> (2012).
40. Palgen, J.-L. et al. Optimize Prime/Boost vaccine strategies: Trained immunity as a new player in the game. *Front. Immunol.* <https://doi.org/10.3389/fimmu.2021.612747> (2021).
41. Bhattacharya, S. et al. Heterologous Prime-Boost with Immunologically Orthogonal Protein Nanoparticles for Peptide Immunofocusing. *bioRxiv* <https://doi.org/10.1101/2024.02.24.581861> (2024).
42. Wang, S. et al. Cross-subtype antibody and cellular immune responses induced by a polyvalent DNA prime-protein boost HIV-1 vaccine in healthy human volunteers. *Vaccine* **26**, 3947–3957. <https://doi.org/10.1016/j.vaccine.2007.12.060> (2008).
43. Lu, S. Heterologous prime-boost vaccination. *Curr. Opin. Immunol.* **21**, 346–351. <https://doi.org/10.1016/j.coi.2009.05.016> (2009).
44. Pflumm, D. et al. Heterologous DNA-prime/protein-boost immunization with a monomeric SARS-CoV-2 spike antigen redundantly trimerizes the trimeric receptor-binding domain structure to induce neutralizing antibodies in old mice. *Front. Immunol.* **14**, 1231274. <https://doi.org/10.3389/fimmu.2023.1231274> (2023).
45. Rahikainen, R. et al. Overcoming symmetry mismatch in vaccine nanoassembly through spontaneous amidation. *Angew Chem Weinheim Bergstr Ger* **133**, 325–334. <https://doi.org/10.1002/ange.202009663> (2021).
46. Joshi, S. et al. Evaluation of immune response to single dose of quadrivalent HPV vaccine at 10-year post-vaccination. *Vaccine* **41**, 236–245. <https://doi.org/10.1016/j.vaccine.2022.11.044> (2023).

47. Hu, Y. M. et al. Safety of an *Escherichia coli*-expressed bivalent human papillomavirus (types 16 and 18) L1 virus-like particle vaccine: An open-label phase I clinical trial. *Hum. Vaccin. Immunother.* **10**, 469–475. <https://doi.org/10.4161/hv.26846> (2014).
48. WHO. *HPV vaccine introduction, Global HPV programme status data* [Internet]. Accessed on 18.03.25. Available at: <https://immunizationdata.who.int/>.
49. Canali, E. et al. A high-performance thioredoxin-based scaffold for peptide immunogen construction: Proof-of-concept testing with a human papillomavirus epitope. *Sci. Rep.* **4**, 4729. <https://doi.org/10.1038/srep04729> (2014).
50. Degn, S. E. & Tolar, P. Towards a unifying model for B-cell receptor triggering. *Nat. Rev. Immunol.* **25**, 77–91. <https://doi.org/10.1038/s41577-024-01073-x> (2025).
51. Bennett, N. R., Zwick, D. B., Courtney, A. H. & Kiessling, L. L. Multivalent antigens for promoting B and T cell activation. *ACS Chem. Biol.* **10**, 1817–1824. <https://doi.org/10.1021/acschembio.5b00239> (2015).
52. Zhao, R. et al. Improvement of the immunogenicity of ESAT-6 via fusion with the dodecameric protein dodecin of *Mycobacterium tuberculosis*. *Microb. Pathog.* **155**, 104890. <https://doi.org/10.1016/j.micpath.2021.104890> (2021).
53. Zhao, X. et al. A safe and potentiated multi-type HPV L2-E7 nanoparticle vaccine with combined prophylactic and therapeutic activity. *NPJ Vaccines* **9**, 119. <https://doi.org/10.1038/s41541-024-00914-z> (2024).
54. Yang, F. et al. Broad neutralization responses against oncogenic human papillomaviruses induced by a minor capsid L2 polytope genetically incorporated into bacterial ferritin nanoparticles. *Front. Immunol.* **11**, 606569. <https://doi.org/10.3389/fimmu.2020.606569> (2020).
55. Kraft, J. C. et al. Antigen- and scaffold-specific antibody responses to protein nanoparticle immunogens. *Cell. Rep. Med.* <https://doi.org/10.1016/j.xcrm.2022.100780> (2022).
56. Veggiani, G., Zakeri, B. & Howarth, M. Superglue from bacteria: Unbreakable bridges for protein nanotechnology. *Trends Biotechnol.* **32**, 506–512. <https://doi.org/10.1016/j.tibtech.2014.08.001> (2014).
57. Zakeri, B. et al. Peptide tag forming a rapid covalent bond to a protein, through engineering a bacterial adhesin. *Proc. Natl. Acad. Sci.* **109** <https://doi.org/10.1073/pnas.1115485109> (2012).
58. Veggiani, G. et al. Programmable polyproteins built using twin peptide superglues. *Proc. Natl. Acad. Sci. U. S. A.* **113**, 1202–1207. <https://doi.org/10.1073/pnas.1519214113> (2016).
59. Kang, H. J. & Baker, E. N. Intramolecular isopeptide bonds: Protein crosslinks built for stress?. *Trends Biochem. Sci.* **36**, 229–237. <https://doi.org/10.1016/j.tibs.2010.09.007> (2011).
60. Tam, H. H. et al. Sustained antigen availability during germinal center initiation enhances antibody responses to vaccination. *Proc. Natl. Acad. Sci. U. S. A.* **113**, E6639–E6648. <https://doi.org/10.1073/pnas.1606050113> (2016).
61. Ols, S. et al. Multivalent antigen display on nanoparticle immunogens increases B cell clonotype diversity and neutralization breadth to pneumoviruses. *Immunity* **56**, 2425–2441 e2414. <https://doi.org/10.1016/j.immuni.2023.08.011> (2023).
62. Seitz, H., Danthony, T., Burkart, F., Ottonello, S. & Muller, M. Influence of oxidation and multimerization on the immunogenicity of a thioredoxin-L2 prophylactic papillomavirus vaccine. *Clin. Vaccine Immunol.* **20**, 1061–1069. <https://doi.org/10.1128/CVI.00195-13> (2013).

Acknowledgements

We would like to thank to Dr. Karsten Richter for electron microscopy analysis. Thanks to Dr. Simone Ottonello for his valuable advices for the study design. Ministry of Education of Turkey provided the scholarship for Ecem Kaplan. The funder had no role in study design, data collection and analysis, decision to publish, or preparation of the manuscript.

Author contributions

EK and MM were the principal contributors for design of the study and manuscript preparation. EK was also responsible to perform production, characterization and immunogenicity evaluation of the tested antigens. FCM, EK, YZ, XZ and HW were responsible to perform animal experiments to test B-cell response and to produce monoclonal antibodies. MN performed electron microscopy analysis. YZ performed the AlphaFold modelling of Trx-8mer-mtDod (Data is not shown). EK, FCM, HW and MM were involved in data analysis, interpretation of experimental findings and manuscript preparation. LV was responsible for production of anti-DogTag and anti-DogCatcher monoclonal antibodies. MM was responsible for acquiring funds. All authors reviewed the draft of the manuscript and approved for submission.

Funding

Open Access funding enabled and organized by Projekt DEAL.

Declarations

Competing interests

The authors declare no competing interests.

ARRIVE statement

All animal experiments were performed and reported in accordance with ARRIVE (Animal Research: Reporting In Vivo Experiments) guidelines.

Additional information

Supplementary Information The online version contains supplementary material available at <https://doi.org/10.1038/s41598-026-42678-7>.

Correspondence and requests for materials should be addressed to M.M.

Reprints and permissions information is available at www.nature.com/reprints.

Publisher's note Springer Nature remains neutral with regard to jurisdictional claims in published maps and institutional affiliations.

Open Access This article is licensed under a Creative Commons Attribution 4.0 International License, which permits use, sharing, adaptation, distribution and reproduction in any medium or format, as long as you give appropriate credit to the original author(s) and the source, provide a link to the Creative Commons licence, and indicate if changes were made. The images or other third party material in this article are included in the article's Creative Commons licence, unless indicated otherwise in a credit line to the material. If material is not included in the article's Creative Commons licence and your intended use is not permitted by statutory regulation or exceeds the permitted use, you will need to obtain permission directly from the copyright holder. To view a copy of this licence, visit <http://creativecommons.org/licenses/by/4.0/>.

© The Author(s) 2026